Numerical Modelling of Cell Dehydration during Cryopreservation

By

Dibya Devismita
(Roll No – 609BM102)

Under the guidance of
Dr. Amitesh Kumar

Thesis submitted in the partial fulfilment of the requirements for the degree of

Master of Technology by Research

in

Biotechnology & Medical Engineering

Department of Biotechnology and Medical Engineering
National Institute of Technology
Rourkela, India

Numerical Modelling of Cell Dehydration during Cryopreservation

By

Dibya Devismita
(Roll No – 609BM102)

Under the guidance of
Dr. Amitesh Kumar

Thesis submitted in the partial fulfilment of the requirements for the degree of

Master of Technology by Research

in

Biotechnology & Medical Engineering

Department of Biotechnology and Medical Engineering
National Institute of Technology
Rourkela, India

NATIONAL INSTITUTE OF TECHNOLOGY
ROURKELA

CERTIFICATE

This is to certify that the thesis entitled "**NUMERICAL MODELLING OF CELL DEHYDRATION DURING CRYOPRESERVATION**" by Mrs. **Dibya Devismita** submitted to the **National Institute of Technology**, Rourkela for the Degree of Master of Technology by research in Biotechnology & Medical Engineering, is a record of bonafide research work, carried out by her in the Department of Biotechnology and Medical Engineering under my supervision. I believe that the thesis fulfils part of the requirements for the award of Master of Technology by research. To the best of my knowledge, the matter embodied in the thesis has not been submitted to any other University / Institute for the award of any Degree or Diploma.

Dr. Amitesh Kumar
Assistant Professor
Dept. of Mechanical Engg.
National Institute of Technology
Rourkela, India

ACKNOWLEDGEMENT

I offer my sincere heartfelt gratitude to Dr Amitesh Kumar, Assistant Professor, Department of Mechanical Engineering for his constant supervision, advice and guidance as well as sharing his professional experiences throughout this project.

I also express my sincere gratitude to Prof. Krishna Pramanik, Head of the Department, Department of Biotechnology and Medical Engineering, for providing valuable departmental facilities and for constantly evaluating me and providing me with insightful suggestions.

I am also thankful to my lab mates Mr. Nakul Dewan, Mr. Karan Bhatt, and Mr. Krishna Kumar, who were a great moral support during my work.

Last, but not the least, I would thank the God and my family, whose love and trust on me has brought at this stage of my life.

Submitted By:

Dibya Devismita
Roll No- 609BM102
Dept. of Biotechnology & Medical Engg.
National Institute of Technology
Rourkela, India

TABLE OF CONTENTS

LIST OF TABLES

LIST OF FIGURES

LIST OF FIGURES

NOMENCLATURE

A_c	Effective membrane surface area
B_{opt}	Optimal Cooling Rate
c_{gi}	Initial concentration of Cryoprotectant
CPA	Cryoprotective Agent
CR	Cooling Rate
ΔH_f	Latent heat of fusion of water
E_{Lp}	Activation energy
L_{pg}	Reference membrane permeability
R	Universal gas constant
SA	Surface area
T_R	Reference temperature
V	Cell volume
V_0	Isotonic volume
V_b	Osmotically inactive volume
v_{cpa}	Molar volume of cryoprotectant
v_w	Molar volume of water
WV	Water Volume

Greek Symbols

φ	Disassociation constant
ρ	Density of water

ABSTRACT

Cryopreservation is a novel and innovative technique for preserving cells or tissues by cooling to sub-zero temperatures. During the process the transport of water takes place across the cell membrane. The chemical potential difference arising due to different concentrations across the cell membrane is responsible for this transport. The water transportation depends on many parameters, e.g. cell level parameters such as membrane permeability to water L_{pg}, activation energy E_{Lp}, and available surface area to water volume ratio SA/WV, the initial concentration of cryoprotective agent (CPA), and the cooling rate. The membrane limited water transport model is utilized to study the effect of above mentioned parameters on the dehydration of cell and an optimal cooling rate is obtained for which one can have maximum viability. Here, the optimal cooling rate is defined as the highest cooling rate for which amount of trapped water inside the cell is equal to 5% of the initial cell water content at the end of preservation process where the end temperature is considered to be -40^0C. The criterion for selecting -40^0C as the end temperature and its effect on the optimal cooling rate have also been discussed in detail. Based on the predicted optimal cooling rate, a correlation is established between the optimal cooling rate, cell level parameters, and the initial concentration of CPA with a goodness of fit 99.6%.

Key words- cryopreservation, optimal cooling rate, activation energy, reference membrane permeability, end temperature, cryoprotectant and initial cryoprotectant concentration.

CHAPTER 1

INTRODUCTION

1.1 INTRODUCTION

Cryobiology is the branch of science that is concerned with the study of living systems ranging from singe cell to entire plants and animals at extremely low temperature. There are many aspects of cryobiology that are important for the fundamental understanding of freezing in living systems but to be very precise, there are two crucial facets namely cryosurgery and cryopreservation which find application in different research disciplines. The former one deals with the destruction of cells selectively while the latter one is used to preserve and store them for longer period of time. With the rapid increase in infertility cases, accidents leading to multiple organ failure and several complications related to healthcare, the study of cryopreservation, its existing limitations and its benefits have become an area of active research. Therefore, a lot of studies need to be carried out by researchers for the refinement of knowledge of the scientific community in this very fascinating field of cryopreservation.

As stated above cryopreservation is a technique using which living cells or tissues can be preserved at a stage called ‘suspended animation’ where all the biological and biochemical activities which lead to cell death are suspended [1]. Though, the act of preservation in low temperature is not that naive but recently it has become a keen area of research among the scientists due to its vast contribution towards preservation and banking of different cell lines and tissue engineered products, transplantation of cells and more importantly in-vitro fertilization. During the process of freezing the cells are stored in liquid nitrogen (LN_2) at a sub-zero temperature (usually at -80°C). The reason why liquid nitrogen is the most preferred cryogenic fluid is due to its low boiling point i.e. −196°C (77 K; −321 °F) which causes rapid freezing on contact with living systems. This

leads to a much wider use of cryopreservation both in medical treatments and scientific research. For medical procedures like transplantation, cells or tissues may be conveniently stored and used later. But in scientific research, cryopreservation will facilitate the archiving of biological samples which shall enable the researchers with new findings. Nowadays, many cells, tissues as well as organs are routinely stored in low temperature and also cryopreservation finds its application in other fields such as food science, plant and animal cold hardiness, ecology and agriculture. Although, this technique has become popular but it has its own limitations; as in real practice a cell may experience various physical stresses and give an equivalent stimulus to counteract that stress. Hence, the biophysical response of a cell and its proper optimization becomes a significant factor in deciding the outcome of the process.

A better cryopreservation protocol needs optimization of certain parameters such as mass transport, phase change temperature, holding time at each step, cooling rate and ice formation. Out of the above mentioned parameters the cooling rate alone is the major deciding parameter during the process of freezing. Also, the temperature after which the cell or tissue is plunged into liquid nitrogen is also important. This temperature is termed as end temperature in this study. Thus, minimizing the destructive effect is essential for the cryopreservation protocol [2]. This goal could be achieved by quantitative knowledge of the biophysical response during freezing of biological systems, after knowing the fact that different cells respond differently when they are exposed to low temperature. And hence, optimization of cryopreservation process for the cells is needed, to preserve them for longer period of time without unsettling their functionality and to achieve maximum viability rate. Apart from these, cryoprotective agents (CPAs) play a key role in

cryopreservation as their addition improves the survival of cells. Addition of these chemicals changes the composition and properties of the intracellular solution by lowering the freezing point, binding water to prevent it freezing at zero degree, and decreasing membrane damages [3].

From the foregoing discussions, it is clearly understood that for the optimization of cryopreservation protocol the following several necessary steps should be considered:

- Storage at liquid nitrogen temperature for a longer period of time
- Addition of adequate amount of CPAs
- Freezing at an optimal cooling rate
- Anticipation of extracellular ice nucleation
- Checking of extra and intracellular ice formation
- Thawing and removal of CPAs.

1.2 REVIEW OF LITERATURE

History says preservation in low temperature had started by the Egyptians for medical treatment in the year 2500 BC and since then with emergence of science and technology it has become a regular practice in today's world.

In 1776 Spallanzani was the first to report about the maintenance of motility of human spermatozoa after exposure to low temperature [4] and then in the year 1866 Mantagazza suggested sperm banks for frozen human semen. But the accidental discovery of glycerol as a cryoprotectant gave a new direction to the field of cryopreservation [5] and till date storage of living systems using ultra-low temperature has been applied successfully to numerous mammalian systems which includes erythrocytes, lymphocytes, gametes, embryos, hepatocytes, bone marrow stem cells, pancreatic tissues [2], mammalian oocytes [6, 7], stem cells [8], rat and human liver slices [9] and engineered tissues [10]. Its applications are also extended in a variety of fields such as food science, plant and animal cold hardiness, ecology and agriculture. But still there are many pros and cons that need to be considered during the low temperature freezing process which will lead us towards establishing a proper cryopreservation protocol resulting in maximum cell viability.

In early 1950s Lovelock suggested that increasing salt concentrations in a cell might cause damages to the cell because of cell dehydration [11]. Mazur in the year 1963 proposed that, the survival of various cells subjected to low temperature is higher when they are cooled slowly. This is due to the decrease in probability of intercellular freezing as it permits the water to leave the cell rapidly to keep protoplasm at its freezing point.

He did the experiment with various mammalian cells with different cooling rates and found that at the cooling rate of 1°C/min the intercellular water content is closer to the equilibrium value. Hence the amount of ice formation at this cooling rate will be less [12]. He also studied the rapidly frozen suspension of yeast cells by differential thermal analysis [13]. Bank and Mazur [14] stated that when cells are cooled at rates exceeding a critical velocity, a decrease in viability is caused by the presence of intracellular ice. The experiment was conducted with yeast cells (*Saccharomyces cerevisiae*) and it was observed that cells cooled at a rate of ~7°C/min showed maximum viability.

In 1972, Mazur et al. measured that the survival of cell is related to the cooling rate and found that post-thaw viability of cells at an intermediate cooling rate is higher than that of faster and slow cooling rate where survival rate is much lower [15]. They also suggested that the injuries associated with fast and slow cooling rate are the consequences of intracellular ice formation (IIF) and excessive dehydration respectively. Muldrew and McGann proposed a hypothesis about the mechanism of intracellular ice formation which occurs due to the osmotic imbalance across the plasma membrane. An indication of this hypothesis is that mathematical models can be used to design protocols to avoid damaging gradients in osmotic pressure, allowing new approaches to preservations of cells, tissues and organs by rapid cooling [16] and later they proposed a mathematical framework which gave an accurate description of the phenomenology of intracellular ice formation [17].

Karlsson et al. in 1994 developed a theoretical model for predicting the kinetics of ice crystallization within the cells during cryopreservation and also studied the effect of glycerol concentration on intracellular crystal growth in mouse oocytes [18]. And further

study on the effect of different cryoprotective additives on intracellular ice formation (IIF) and extracellular ice formulation (EIF) was accomplished by Mazur et al. [6]. As discussed earlier these cryoprotectants act as a solvent to dilute the intracellular and extracellular solute concentrations when water is removed, thus protecting the cell from solution effects injuries and they also reduce the rate of formation of ice crystals [2]. Depending on their ability to transport across cell membrane, cryoprotective agents (CPAs) are categorized into penetrating, e.g. glycerol and Dimethyl Sulphoxide (DMSO), Propylene Glycol (PG) and non-penetrating, e.g. lactose and trehalose. And the selection of CPA to be used during freezing process entirely depends upon the property (type) of the substance (cell) to be cryopreserved. Currently, glycerol and DMSO are the most commonly used CPAs because the effectiveness is much higher in their cases as compared to other CPAs for most of the substances. Usually, glycerol and DMSO are used 5-10% (v/v) in concentrations. Prior to being added to the cell suspension, CPAs should be diluted to the desired concentration in fresh growth media. This procedure reduces the potential toxic effects as higher concentration of cryoprotectants could be hazardous.

A new era of cryopreservation was started when scientists discovered the use of differential scanning calorimeter (DSC) and Cryomicroscope. Using DSC the water transport can be measured in a cellular system during freezing. But it has some limitations, that it requires a prior knowledge about the biophysical parameters such as the initial volume, osmotically inactive cell volume and surface area, and the technique alone cannot determine whether the heat released from supercooled cellular water is due to dehydration or intracellular ice formation. Cryomicroscopy was used to address these

limitations [19-23]. Using this technique the researchers investigated the effect of cooling rate on the biophysical parameters for different cell lines and formulated the optimal cooling rate for them [24-26]. Other than this, cell parameters were also studied using optical microscopy [27] and electron paramagnetic resonance method [28].

Apart from all the experimental approaches, cryopreservation became more promising as well as interesting when researchers started developing the mathematical models for cell response to low temperature freezing. This helped in modeling rational designs and optimization of protocols for cell and tissue cryopreservation. As the residual water content affects both the IIF and solution effects damage hence the mathematical model includes the description for the mass transport process that governs the redistribution of intracellular water. The mass transport Biot number (Bi) is used to differentiate the type of mass transport that occurs across the cell membrane during the freezing process. The water transport is a diffusion-limited process when Bi » 1, and it becomes membrane-limited when Bi « 1. Most of the former models were developed assuming the water transport to be membrane limited process.

In 1933, Jacobs proposed a two-parameter approach for membrane transport, one parameter describing the membrane permeability to water and other parameter describing the membrane permeability to solute [29]. Later, a third parameter was added by Kedem and Katchalsky to account for the co-transport of species, e.g. the coupled transport of water and solute through the same membrane channel [30]. In 1963, Mazur proposed a theoretical model for membrane-limited water transport for freezing of cells assuming that the CPA flux to be negligible [13] and it was later modified by Levin et al. [31] who also included the effect of CPA. Though it was reported earlier that mass transport will be

membrane limited for low Biot number but later the concept was modified illustrating that mass transfer will be diffusion-limited during the thawing process from the cryopreserved state, even for the cell types that are having low Biot numbers during the freezing process [32]. But, for this study all the simulations were done by using the membrane limited water transport model assuming that cell contains only water and salt within it. A detailed description has been given in later part of this chapter.

1.3 MECHANISM OF CELL DEHYDRATION

The cryopreservation process involves complex biophysical responses of cells and tissues which are not clearly understood. A typical cell consists of water, salt, proteins and other macro-molecules. But, water is considered to be the major component of all living systems and also helps in carrying out the biological and biochemical processes within the cellular environment. It is extremely important to understand the mechanism of cell dehydration.

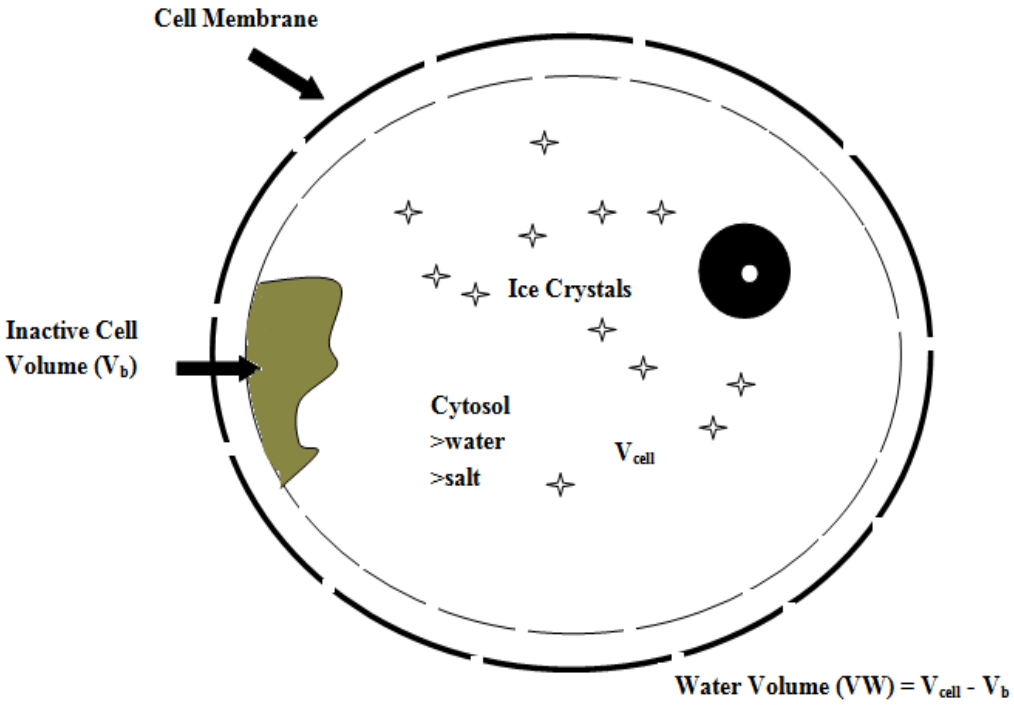

Figure 1: Schematic diagram of a Cell during freezing process

Fig. 1 represents the schematic diagram of a cell during the freezing process. During this process both the cell and its surrounding medium remain unfrozen, both because of super-cooling and because of the depression of freezing point by the protective solutes that are present in the system. As stated by Mazur [2], within a temperature range of -5^0C

to -15^{0}C, ice forms in the external medium either spontaneously or as a result of seeding the solution with ice crystals. However, the cell contents remain unfrozen and supercooled, probably because the plasma membrane blocks the growth of ice crystals into the cytoplasm. As a result the water inside the cell gets supercooled and the supercooled water has comparatively higher chemical potential than that of the partially frozen solution outside the cell. This generates a potential difference across cell membrane and for sustaining equilibrium water flows out of the cell. Thus the intracellular water content decreases, intra and extracellular solute concentrate [2]. And these are the occurrences of "*solution effect"*, which specifically occur when cell suspension at a constant pressure is exposed to extreme low temperature for longer time duration [33]. Subsequently, solutes precipitate below the eutectic point of the system [13, 34, 35]. Here cooling rate plays a vital role in regulating the exposure time of the cell to these solution effects, which means if the cooling rate is slow then the cell exposure to these effects is longer.

In summary, how the cells will attain their equilibrium mainly depends on the rate at which they are cooled. Because when the cooling rate is slow or the permeability to water is high then the cells will equilibrate themselves by transferring the intracellular water to the external ice or in simple words cells will dehydrate. And on the other hand, when they are cooled rapidly or the permeability to water is low they will equilibrate by intracellular freezing and it is suggested that the lethal event in rapidly cooled cells is the growth of intracellular ice crystals rather than their initial formation [34], [36-38]. The resulting events of slow and rapid cooling rates are presented in figure 2 and figure 3.

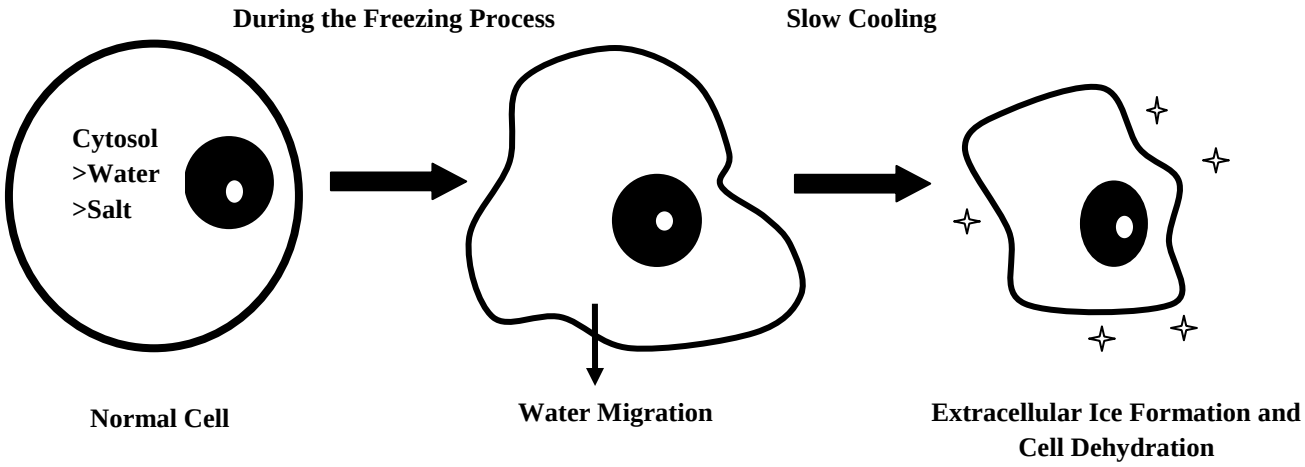

Figure 2: Schematic diagram of a Cell during Slow freezing process

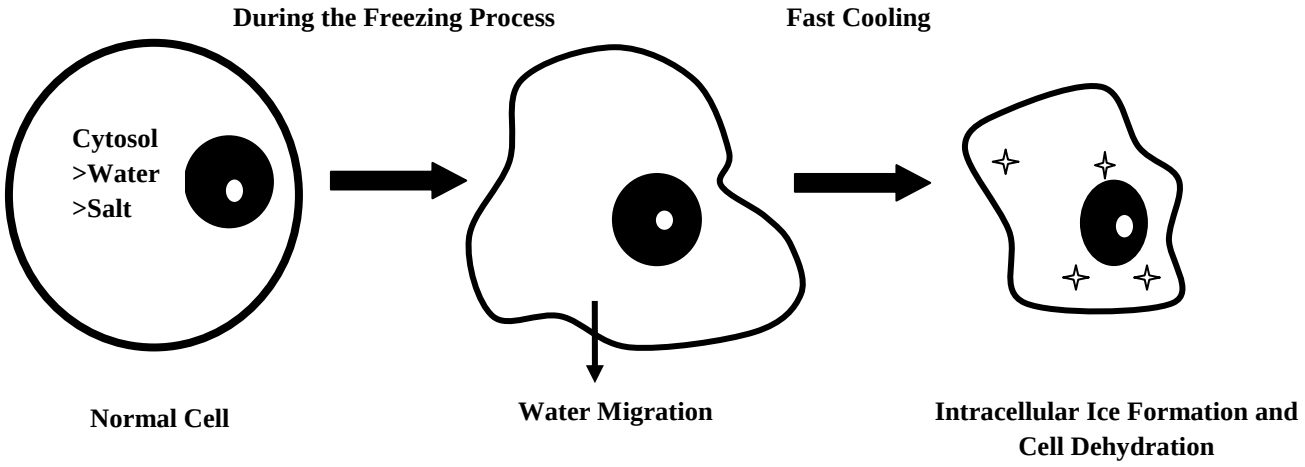

Figure 3: Schematic diagram of a Cell during Fast freezing process

Optimal Cooling Rate

It is clear from the above discussions cooling velocity affects the physiochemical events in the cell during freezing and, so, their rate of survival after the thawing process. This indicates that there should be an optimal cooling rate at which the cell neither encounters damage due to intracellular ice formation nor it experiences solution effect due to excessive dehydration. Figure 4 shows a schematic diagram for this case.

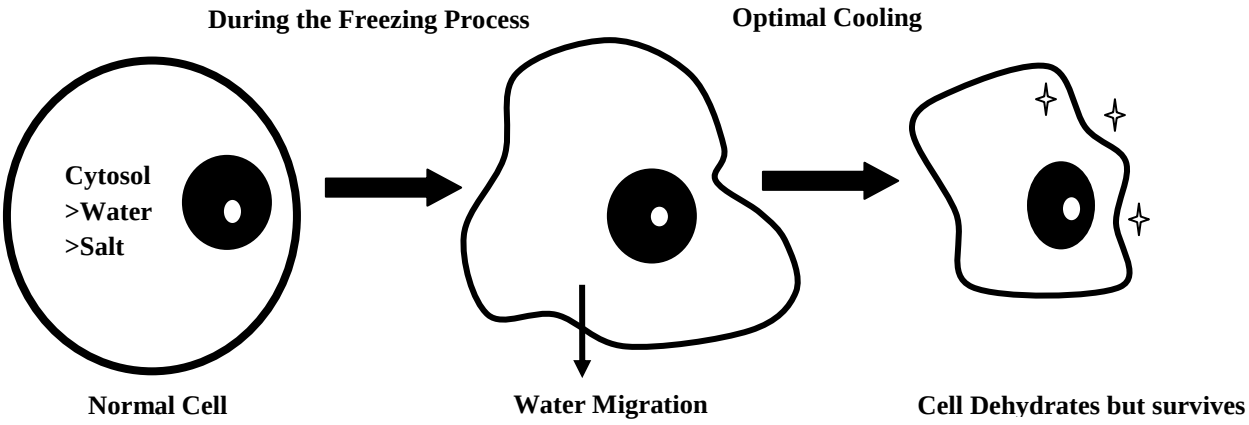

Figure 4: Schematic diagram of a Cell during Optimal Cooling Rate

Action of Cryoprotectant (CPA)

Now it is clear that cooling rate at optimum level helps in cell survival during cryopreservation but as discussed earlier, cryoprotectant (CPA) plays a major role in increasing the rate of cell viability during the preservation process. Basically, CPA is a

chemical that dissolves in water and helps in lowering the freezing point of water. It is used to have higher post-thaw viability [39]. Its effect is schematically shown in figure 5.

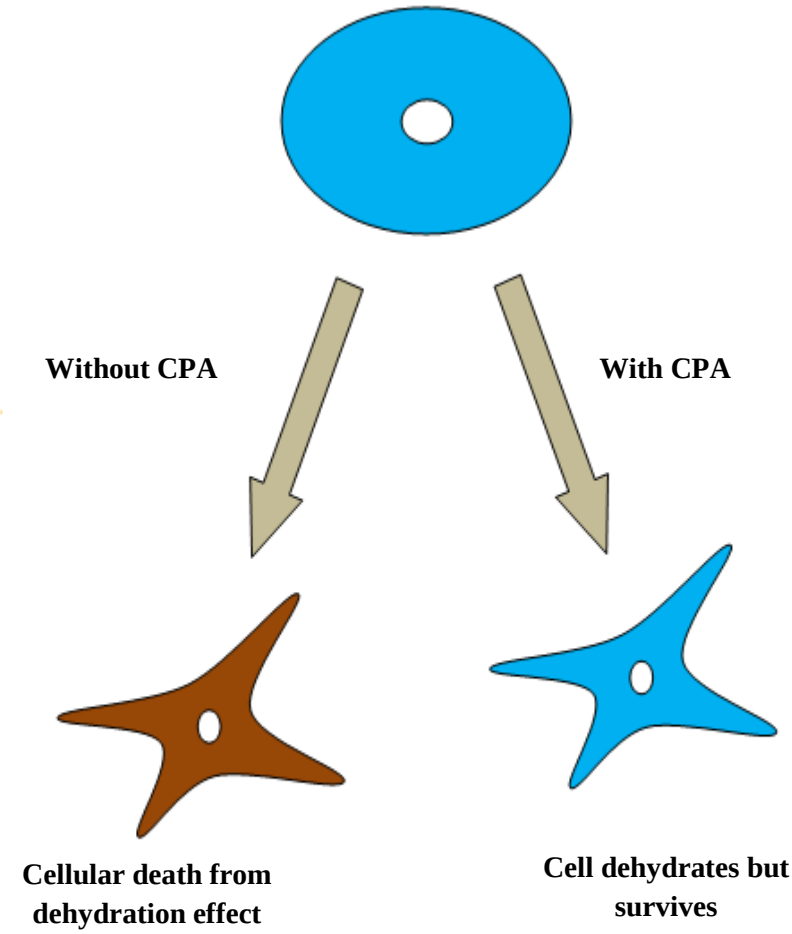

Figure 5: Effect of CPA on cell during Cryopreservation

When the temperature is lowered during the cryopreservation process, growth of ice compresses the cells into smaller pockets of unfrozen liquid and presence of CPAs helps in increasing the size of the pockets and thus reducing the frequency of damage from both forms of freezing injuries: mechanical damage from ice and excessive concentration of salt. A concentration of 5% to 15% is usually required to permit the survival of the cells for longer time duration because amount greater than this causes toxicity. When

more amount of cryoprotectant is added to the cells than required then it forms potentially toxic formaldehyde by non-enzymatic reactions. And, these reactions are the consequences of formation of hydrogen bonds with the proteins. This leads to unfolding and finally protein denaturation [40], which is definitely not in the favour of cell survival. The other adverse effect of adding cryoprotectant in higher concentration is that it may disintegrate the DNA and thus reduces the activity of the cell during cryopreservation. It has been found that cryoprotectants like glycerol and DMSO are the two additives which cause least damage to the cells and helps in preservation for longer duration. More detailed discussion has been done in chapter 3 regarding the effect of CPA on optimal cooling rate.

1.4 MATHEMATICAL MODELLING

Though water and salt (NaCl) are the major constituents of a cell but it also contains proteins and macromolecules within it. However, these proteins and macromolecules, that are present in the cytosol, are considered as inactive to the physical processes that are going on during the freezing process. And hence the total cell volume is thus $V_{cell} = V_0 + V_b$ where V_0 is the isotonic cell volume that includes the cytosolic solution and V_b is the inactive cell volume (as shown in Figure 1). During cryopreservation, the water transport within a cell is driven by a chemical potential difference between the intracellular and extracellular solutions. The intracellular water moves towards the extracellular solution which leads to the volumetric shrinkage of the cell as a result of this potential difference. Analysing this, Kedem and Katchalsky [30] first proposed the water transport model considering water and solute transport across the cell membrane. They proposed two differential equations for water and CPA fluxes through the cell membrane. But, if the CPA flux is negligible as compared to the water flux then the Kedem-Katchalsky model reduces itself where only water transportation occurs as stated by Mazur [12] which was later modified by Levin et al. [31] assuming that the permeability of membrane depends only on temperature.

The water transport model is postulated considering the assumptions described below:

- The biological cell is an ideal open thermodynamic system where intra and extracellular compartments are well-mixed, and separated by a semi-permeable membrane which only allows water transportation;
- The cytosol has uniform temperature distribution;

- The chemical potential difference across the cell membrane is proportional to the ratio of partial pressures;
- Intracellular solution is dilute and ideal;
- Volume of the cell is equivalent to the volume of the sphere ($V= 4\pi r^3/3$) with infinite extracellular space.
- Effective membrane surface area ($A_c= 4\pi r^2$) is constant for water transport where r is the cell radius.
- And the membrane permeability is temperature dependent.

This ultimately derives the simplest form of water transport model as,

$$\frac{dV}{dT} = -\frac{L_p A_c RT}{B v_w}\left[ln\frac{a_i^w}{a_o^w}\right] \qquad (1)$$

where V is the cell volume, T is the absolute temperature, L_p is the permeability of the membrane to water, R is the gas constant, B is the constant cooling rate, A_c is the effective membrane surface area available for water transport, $a_i^w and\, a_o^w$ are the chemical potentials for intracellular and extracellular fluids respectively. Quantitative use of the above thermodynamic model requires a more complete specification of the chemical activities of the extracellular and the intracellular solutions, along with the membrane water permeability.

The extracellular solution is assumed to be a binary system consisting of liquid and solid i.e. water and salt (NaCl) and using Gibbs-Helmholtz equation, the extracellular activity can be related to the temperature as follows,

$$\frac{\partial(\ln a_w)}{\partial T} = \frac{\Delta H_f}{RT^2} \qquad (2)$$

Where ΔH_f is the latent heat of fusion of water and it is assumed to be constant with a value 335 mJ/mg. Integrating equation (2) we can get the expression for extracellular activity which is given as,

$$\ln a_w = \frac{\Delta H_f}{R}\left[\frac{1}{T_R} - \frac{1}{T}\right] \qquad (3)$$

Here T_R is the reference temperature (T_R =273.15 K). Since the intracellular solution is assumed to be ideal so the internal water becomes equal to the mole fraction of water and can be represented as,

$$a_w^i = X_w^i \qquad (4)$$

Regardless of any circumstances the cell will be always left with the osmotically inactive cell volume (V_b). Hence considering this factor as well as neglecting the volume of cell membrane the mole fraction of intracellular water converts as follows,

$$X_w^i = \frac{(V - V_b)}{(V - V_b) + \varphi_s n_s v_w} \qquad (5)$$

Where V is the cell volume, v_w is the partial molar volume of water, φ_s is the disassociation constant for sodium chloride, n_s is the number of moles of solutes in the cell as calculated from initial cell osmolarity and the total osmotically active cell water volume ($V_o - V_b$), where V_o is the initial isotonic cell volume, and V_b is the osmotically inactive cell volume as discussed earlier.

Substituting the values of equation (3) and (5) in equation (1) finally water transport model is given as,

$$\frac{dV}{dT} = -\frac{L_p A_c RT}{B v_w}\left[ln\frac{(V - V_b)}{(V - V_b + \varphi_s n_s v_w)} - \frac{\Delta H_f v_w \rho}{R}\left(\frac{1}{T_R} - \frac{1}{T}\right)\right] \qquad (6)$$

And this was later modified by Karlsson et al. [18] to incorporate the presence of CPA and the equation is given as,

$$\frac{dV}{dT} = -\frac{L_p A_c RT}{B v_w}\left[ln\frac{\left(V - V_b - n_{cpa} v_{cpa}\right)/v_w}{\left(V - V_b - n_{cpa} v_{cpa}\right)/v_w + \left(\varphi_s n_s + n_{cpa}\right)} - \frac{\Delta H_f v_w \rho}{R}\left(\frac{1}{T_R} - \frac{1}{T}\right)\right] \qquad (7)$$

Where L_p is defined by Levin et al [31] as,

$$L_p = L_{pg}\, exp\left[-\frac{E_{Lp}}{R}\left(\frac{1}{T} - \frac{1}{T_R}\right)\right] \qquad (8)$$

L_p is an Arrhenius function of L_{pg} and E_{Lp}, where L_{pg} is the permeability of the membrane to water at a reference temperature (T_R=273.15 K) and E_{Lp} is the apparent activation energy for the reference membrane permeability. With this water transport model, the volume changes of cells during the whole process could be monitored and used for further dynamic analysis of the biophysical process occurred during freezing and thawing, if the membrane parameters are known a priori.

1.5 OBJECTIVE

It has been noticed that the residual water content has a very significant role during the freezing process and depending upon the cooling rate it may either lead to the formation of intracellular ice or cell dehydration which is definitely having an adverse effect on cell viability. But, the cell injury can be minimized by cooling it with an optimal cooling rate. It is observed that not only the cell level parameters (such as activation energy: E_{Lp}, membrane permeability to water: L_{pg}, and surface area to water volume ratio: SA/WV) but also the initial concentration of cryoprotective agent (CPA) influence the optimal cooling rate of cryopreservation technique. Hence, study of the effect of these parameters on the optimal cooling rate is necessary.

This research is mainly divided into two parts. The first part focuses on the prediction of optimal cooling rate when the cells are cryopreserved in the absence of a cryoprotective agent. The predicted optimal cooling rate is compared with the published optimal cooling rate for certain cells. Also, a correlation is developed which predicts the relation between the amount of intracellular ice formation and the cooling rate of cryopreservation process.

The second part focuses on the effect of the concentration of cryoprotective agent on the optimal cooling rate. A thorough investigation is carried out to develop a general correlation for optimal cooling rate which depends on the cell level parameters and the concentration of cryoprotective agent.

CHAPTER 2

EFFECT OF COOLING RATE ON CELL DEHYDRATION

2.1 INTODUCTION

As explained in first chapter, water transportation occurs across the cell membrane due to the potential difference that arises between the partially frozen intracellular water and the extracellular solution. And, depending upon the cooling rate the cells will either get dehydrated which is due to slow cooling rate or will form intracellular ice which is due to the fast cooling rate. These two drawbacks can be overcome when the cell is cooled with an optimum cooling rate which ultimately provides the maximum cell survival rate. Hence, the effect of different cell level parameters on optimal cooling rate has been discussed elaborately in this chapter.

It should be noted that there are two important parameters, apart from the biophysical properties of the cell, which influence the prediction of optimal cooling rate. These parameters are: the amount of intracellular water trapped inside the cell and the end temperature of the freezing process. These two parameters along with the others are described below.

End Temperature:

As discussed earlier, when temperature of the cell falls below the equilibrium temperature, ice formation starts. In this study, the temperature at which ice nucleation commences is termed as end temperature. While predicting optimal cryopreservation protocol for maximum viability the choice of end temperature is critical. Therefore, the investigators varied the end temperature from -10 ^{0}C to -196 ^{0}C to study its effect on the cell response. But, at very low temperature (at -196^{0}C) cell does not have that much thermal energy to carry out any chemical reaction rather it undergoes photo-physical

events such as formation of free radical which eventually leads to DNA disintegration [42, 43]. So, later on an intermediate temperature range was chosen (i.e. from -15^0C to -60^0C) for analysing the effect during freezing [2]. But, for this study the end temperature is considered to be -40^0C; the reason for selecting -40^0C as the end temperature is discussed in detail in the following section.

Trapped Water:

It has already been discussed that trapped water has a very important role during cryopreservation, as fate of the cell is dependent upon how much water is trapped within a cell when it is exposed to low temperature. Usually, 5-10% of initial water volume should be trapped inside the cell at the end of the preservation protocol so that the trapped water could be utilized to start the biochemical and biological activities of the cell during thawing process. However, in this study, it has been assumed that 5% of the initial amount of intracellular water is trapped inside the cell at the end of the preservation process. It is to be noted that all the cell volume shrinkage data are obtained by considering the above mentioned assumptions and the effect of different cell level parameters on the optimal cooling rate is studied.

Optimal Cooling Rate:

The optimal cooling rate is described as the cooling rate which is neither too high nor too low and stores the biological samples for maximum time span. Because, a minor deviation in predicting the optimal cooling rate can reduce the post-thaw viability of cells either by inducing the intracellular ice formation during the freezing process or by solute damage [1]. The optimal cooling rate depends upon different cell-level parameters such

as L_{pg}, E_{Lp}, SA/WV (where SA is the available membrane surface area and WV is the initial intracellular water volume denoted as $WV = V_0 - V_b$). It should be noted here that the cell parameters, V_0, V_b, and A_c are incorporated into a single term SA/WV.

Undercooling:

Another consequence of the low temperature freezing is the undercooling, which is defined as the difference in temperature of the cytoplasm and the equilibrium temperature of the intracellular solution. At the onset of cooling, the biological systems are in equilibrium with the external solution which results in zero undercooling. But when the freezing process starts water comes out of the cell to maintain the equilibrium and cell experiences undercooling depending on the relative strength of the rate at which the temperature of the cytoplasm decreases and the rate at which water gets transported across the cell membrane. Thus, rate of water efflux has a significant effect on the amount of undercooling observed in the cytosol.

2.2 GOVERING EQUATION

Incorporating the above mentioned parameters Mazur [12] proposed a theoretical model for water transportation across the cell membrane without cryoprotectant which was later modified by Levin et al. [31] and is given as (as mentioned in chapter 1, Equation 6),

$$\frac{dV}{dT} = -\frac{L_p A_c RT}{B v_w}\left[ln\frac{(V - V_b)}{(V - V_b + \varphi_s n_s v_w)} - \frac{\Delta H_f v_w \rho}{R}\left(\frac{1}{T_R} - \frac{1}{T}\right)\right] \qquad (6)$$

where V is the cell volume, T is the absolute temperature, L_p is the permeability of membrane to water, R is the gas constant ($8.02\times10^{13}\mu m^3 - atm/mol\,K$), B is the constant cooling rate, A_c is the effective membrane surface area available for water transport, v_w is the partial molar volume of water ($18\times10^{12}\mu m^3/mole$) , φ_s is the disassociation constant for sodium chloride (2); n_s is the number of moles of salt in the cell as calculated from initial cell osmolarity and the total osmotically active cell water volume ($V_o - V_b$), V_o is the initial isotonic cell volume, and V_b is the osmotically inactive cell volume, ΔH_f is the latent heat of fusion of water (335 J/gm), ρ is the density of water (1000 Kg/m^3) . The permeability of membrane to water, L_p, is given as below (as mentioned in chapter 1, Equation 8),

$$L_p = L_{pg}\, exp\left[-\frac{E_{Lp}}{R}\left(\frac{1}{T} - \frac{1}{T_R}\right)\right] \qquad (8)$$

It is to be noted that L_p is an Arrhenius function of L_{pg} and E_{Lp}, where L_{pg} is the permeability of the membrane to water at a reference temperature (T_R=273.15 K) and E_{Lp} is the apparent activation energy for the reference membrane permeability. Although, different cells have different biophysical properties but, if the parameters are known a priori then the optimal cooling rate can be calculated for a particular cell by solving the above two equations.

2.3 NUMERICAL APPROACH

Literature survey reveals that fourth order Runge-Kutta method gives better accuracy than the other existing methods. Therefore, the above mentioned equation is solved using fourth order Runge-Kutta method to predict the optimal cooling rate. In the equations, the important input parameters are: reference membrane permeability L_{pg}, activation energy E_{Lp}, available surface area to water volume ratio SA/WV. The input parameters are varied in the range of 20 Kcal/mole $\leq E_{Lp} \leq$ 80 Kcal/mole, 0.001 μm/min-atm $\leq L_{pg} \leq$ 10 μm/min-atm, and 0.001 $\mu m^{-1} \leq$ SA/WV $\leq$ 10 μm^{-1}. The salt concentration is taken equal to 0.142M.

Initial conditions for numerical solution:

Considering the cell as a sphere of diameter D, initial isotonic cell volume (V_0) can be written as:

$$V_0 = WV + v_b = {\pi D^3}/{6}$$

As v_b can be replaced as fraction of initial isotonic cell volume (fV_0), hence the above equation can be written as:

$$WV + fV_0 = {\pi D^3}/{6}$$

$$WV = (1 - f)V_0$$

$$WV = (1 - f)\frac{\pi D^3}{6}$$

Again it is known that surface area (SA) = πD^2

$$SA/WV = \frac{6}{(1-f)D}$$

$$D = \frac{6}{(1-f)\,SA/WV}$$

If SA/WV is expressed in μm^{-1}, then

$$D = \frac{6 \times 10^{-6}}{(1-f)\,SA/WV}\ m$$

Using the value of D, cell volume and cell surface area can be calculated.

It has been assumed that initially the cell is in isotonic condition. Hence, the left part of Eq. 6 will be zero; this fact is utilised to obtain the initial condition of temperature, T_0. Equating equation 6 to zero gives,

$$-\frac{L_p A_c RT}{B v_w}\left[ln\frac{(V-V_b)}{(V-V_b+\varphi_s n_s v_w)} - \frac{\Delta H_f v_w \rho}{R}\left(\frac{1}{T_R}-\frac{1}{T}\right)\right] = 0$$

$$T = T_0 = \frac{1}{\frac{1}{T_R} - \frac{R}{\Delta H_f v_w \rho}\ ln\frac{(V-V_b)}{(V-V_b+\varphi_s n_s v_w)}}$$

Incorporating all the other values mentioned in section 2.2, T_0 can be calculated from the above relation.

Algorithm for fourth order Runge-Kutta method:

Equation 6 can be cast into $V' = f(T, V)$ with the initial conditions for V with respect to the temperature T, i.e. $V = V_0$ when $T = T_0$. Then, fourth order Runge-Kutta method gives

$$V_1 = h\, f\left(T_0, V_0\right)$$

$$V_2 = h\, f\left(T_0 + \frac{h}{2}, V_0 + \frac{V_1}{2}\right)$$

$$V_3 = h\, f\left(T_0 + \frac{h}{2}, V_0 + \frac{V_2}{2}\right)$$

$$V_4 = h\, f\left(T_0 + h, V_0 + V_3\right)$$

In the above equations *h* is step size of temperature, which is taken as 0.00001 K to 0.001 K depending on the problem at hand. The above step is obtained by satisfying the stability criteria of fourth order Runge-Kutta method as proposed by Liniger [44] and Karim [45]. Finally, the next estimate of *V* is obtained by weighted average of the above four quantities as,

$$V_{new} = V_{old} + \frac{1}{6}\left(V_1 + 2V_2 + 2V_3 + V_4\right)$$

2.4 RESULTS & DISCUSSION

As mentioned earlier L_p, E_{Lp} and SA/WV are the three cell dependent parameters along with the concentration of CPA which influence the cell response during cryopreservation. Therefore, the exhaustive study has been carried out to quantify the effect of these parameters on the optimal cooling rate. The optimal cooling rate is obtained with an assumption of 5% of trapped intracellular water inside the cell and an end temperature of -40^0C.

It is observed that the prediction of optimal cooling rate is highly dependent on the end temperature of the cryopreservation process. Therefore, the selection of end temperature is critically assessed. Figure 2.1 shows the variation of normalised cell volume change

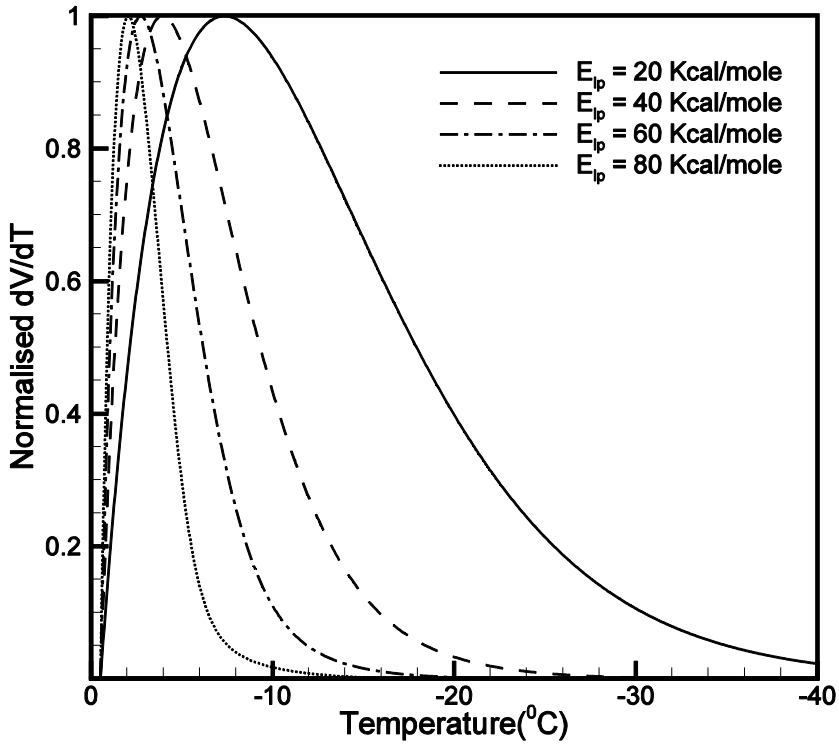

Figure 2.1: Effect of activation energy on cell volume shrinkage rate

with respect to temperature for different values of activation energies. The cell volume change with respect to temperature is normalised by the maximum value. It should be noted that when activation energy is greater than 20 Kcal/mole then the normalised cell volume change with respect to temperature is almost zero for an end temperature of -22^0C. This value is around -10^0C and -15^0C for the activation energy of 60 Kcal/mole and 80 Kcal/mole respectively. The zero value of normalised cell volume change with respect to temperature indicates that the water efflux has stopped and, thereafter, the trapped water inside the cytosol gets converted into ice. Therefore, selection of -15^0C as the end temperature is justified for those cells whose activation energy is greater than or equal to 40 Kcal/mole. It should be noted here that a similar study has also been performed by Thirumala and Devireddy [46] where they have used -15^0C as the end temperature for the prediction of optimal cooling rate. However, if the activation energy is less than or equal to 20 Kcal/mole (which is usually the case with most of the cell lines), the normalised volume change with respect to temperature is not zero at a temperature of -20^0C rather it is almost zero at an end temperature of -40^0C. This effect is more clearly understood from figure 2.2 which shows the variation of optimal cooling rate with the selection of end temperature. It is clear that the optimal cooling rate is independent of end temperature, after -15^0C, when the activation energy is greater than or equal to 40 Kcal/mole. But, for activation energy of 20 Kcal/mole, the optimal cooling rate varies till an end temperature of -40^0C.

The above discussion justifies our assumption of the selection of -40^0C as the end temperature for predicting optimal cooling rate. The literature survey also suggests that in the cells like yeast and human RBC water remains super-cooled to between -30^0C and -40^0C in the absence of external ice [47, 48]. The same

observation is also noticed in higher plant cells which can be super cooled to -40^{0}C [49] without ice nucleation inside the cytoplasm. From here now onwards, -40^{0}C temperature is considered as the end temperature for predicting the optimal cooling rate.

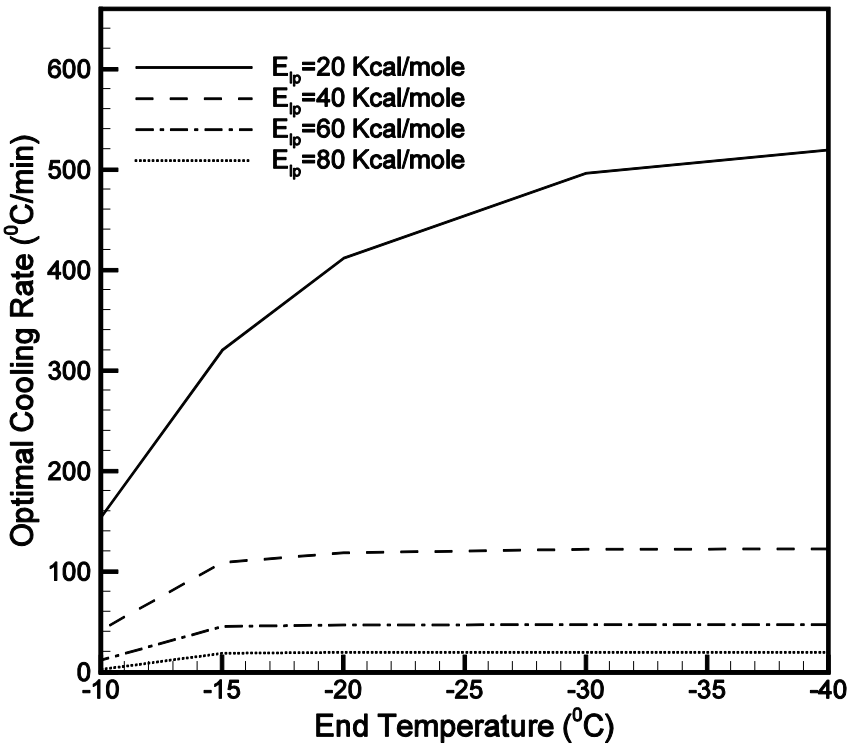

Figure 2.2: Effect of end temperature on optimal cooling rate

Figure 2.3 depicts the variation of normalised water volume with different activation energies when the cells are cooled with an optimal cooling rate. The water volume is normalised by the initial osmotically active water volume. Since the cells are cooled with an optimal cooling rate, as expected, the end volume of trapped water is 5% irrespective of the activation energy. Also, with the increase in activation energy the lower limit of intracellular water content, i.e. 5% is reached much earlier.

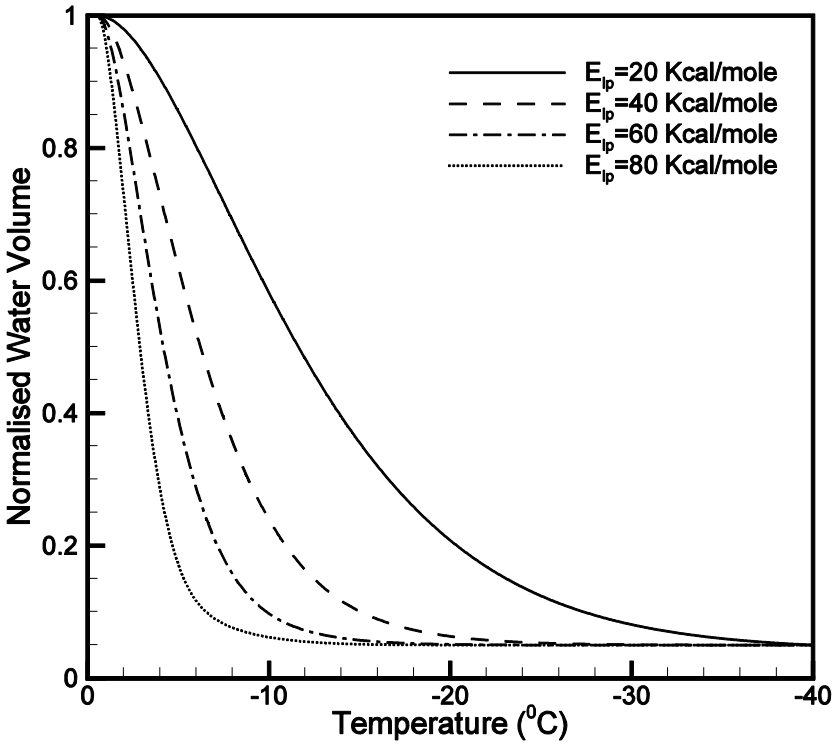

Figure 2.3: Variation of normalised water volume with activation energy at optimal cooling rate

In figure 2.4, the normalised water volume and the temperature are plotted against y-axis and x-axis respectively. To quantify the effect of membrane permeability (L_{pg}) and activation energy (E_{Lp}) on the volume response of the cell four combinations of L_{pg} and E_{Lp} values are selected. For the symbols (∇, O) the value of activation energy is kept fixed at 80 Kcal/mole and the value of reference membrane permeability is varied as 10 and 0.005 µm/min-atm. To our surprise, a single curve is obtained as the variation of normalised cell volume with temperature when the cells, with the above mentioned parameters, are cooled with optimal cooling rate. The similar characteristics are observed when the value of activation energy is changed to 20 Kcal/mole keeping other parameters same. In the figure, the symbols (Δ, □) represent

the variation for this condition. It implies that the variation of normalised water volume at the optimal cooling rate is independent of the reference membrane permeability keeping other parameters same.

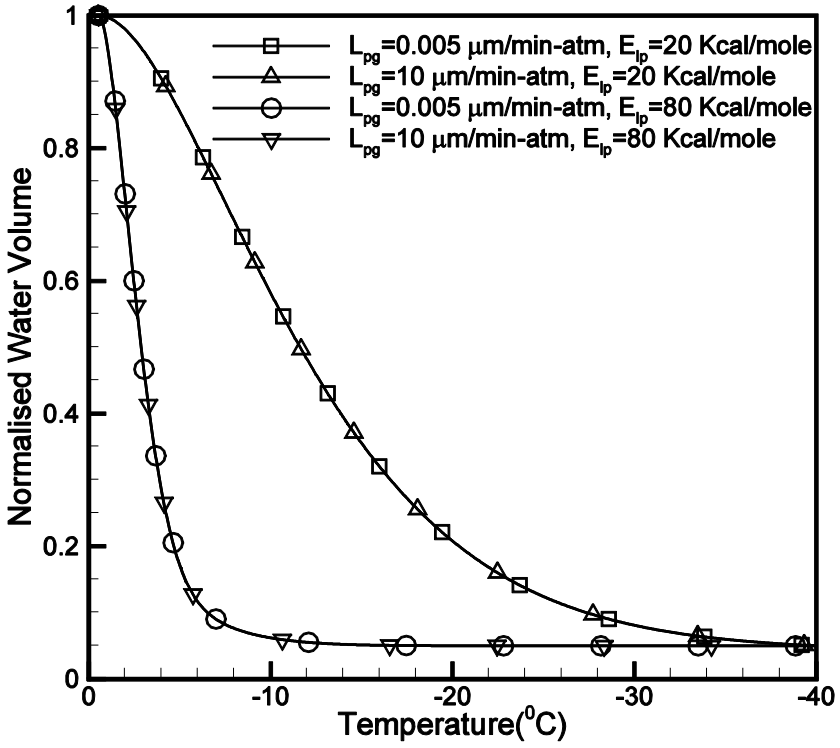

Figure 2.4: Effect of activation energy and reference membrane permeability on normalised water volume at optimal cooling rate

Figure 2.5 shows the variation of undercooling and normalised water volume with temperature for cells with activation energies of 20 Kcal/mole (A) and 80 Kcal/mole. It is noted that these variations are taking place when the cells are cooled with optimal cooling rates. For this study, the available surface area to volume ratio (SA/WV) is taken as 1 μm^{-1} and L_{pg}=1μm/min-atm. For a smaller value of activation energy, i.e. E_{Lp}=20 Kcal/mole, it can be seen that as the water efflux increases the amount of undercooling also increases monotonically (see figure 2.5 A) and

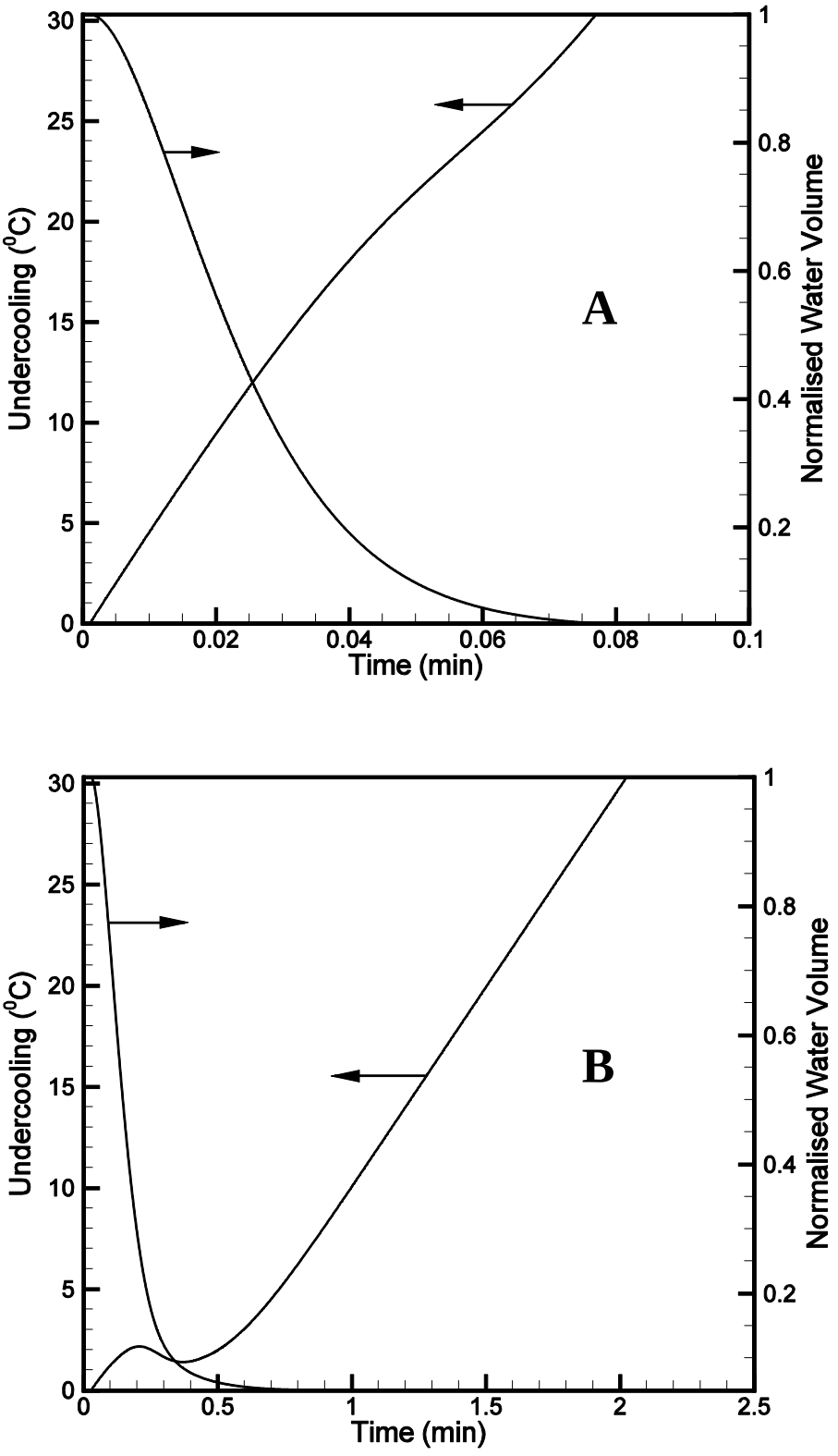

Figure 2.5: Effect of undercooling on normalised water volume at E_{Lp}=20Kcal/mole (A) and E_{Lp}=80Kcal/mole (B)

the undercooling of cytoplasm reaches its maximum value when all the water gets transported across the cell membrane leaving behind only the 5% of the initial intracellular water trapped inside the cell. It takes almost 0.07 minutes to reach this state; after this time, the increase in undercooling is linear. This is owing to the fact that there is no change in cell water volume after this time. Therefore, the temperature of the cytoplasm decreases in accordance with the change in temperature of the system. But, when the activation energy is changed to 80 Kcal/mole, the trend is entirely different (see figure 2.5 B). Now, the value of undercooling first increases, then decreases and again increases with increase in time. It should be noted here that the degree of undercooling depends on two factors: the rate at which the temperature of the cytosol decreases and the rate at which the freezing point of cytosolic water gets depressed due to the efflux of intracellular water. The relative strength of these two phenomena decides whether the undercooling should increase or decrease. For the higher value of activation energy, all the water volume gets driven out within 0.65 minutes of the freezing process while it is 0.07 minutes for the cell with lower value of activation energy.

The effect of reference membrane permeability on optimal cooling rate for different activation energies is shown in figure 2.6. The reference membrane permeability is varied between 0.001μm/min-atm and 4.0μm/min-atm and the activation energy is considered as 20 Kcal/mole and 40 Kcal/mole. It is clear that the optimal cooling rate is varying linearly with reference membrane permeability irrespective of the activation energy keeping the other parameters same. It should be noted here that similar variation is also observed for higher activation energies. Hence, the results for higher activation energies are not presented. This linear behavior can be interpreted from equation 6 which shows a linear dependency of cooling rate on

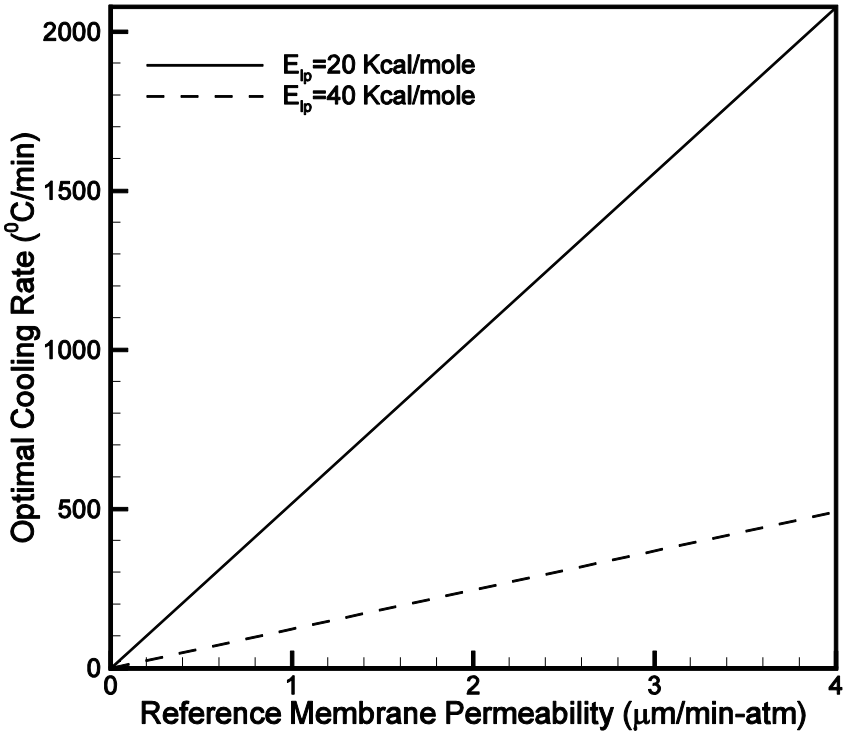

Figure 2.6: Effect of reference membrane permeability on optimal cooling rate

the reference membrane permeability. Although the variation is linear, however, the optimal cooling rate decreases with increase in the activation energy. It should be noted here that because of the linear dependency, the optimal cooling rate is obtained with L_{pg}=1.0μm/min-atm. Therefore, to obtain the actual optimal cooling rate for a particular cell, the predicted optimal cooling rate has to be multiplied with the actual reference membrane permeability of the cell.

In figure 2.7, the predicted optimal cooling rate has been plotted as a function of surface area to volume ratio (SA/WV) at different E_{Lp} values. The value of reference membrane permeability L_{pg} is kept fixed at 1μm/min-atm. It is interesting to observe that optimal cooling rate is varying linearly with the surface area to water volume ratio SA/WV, like it varied with the reference membrane permeability parameter. It can be seen that for a given value of surface area to volume

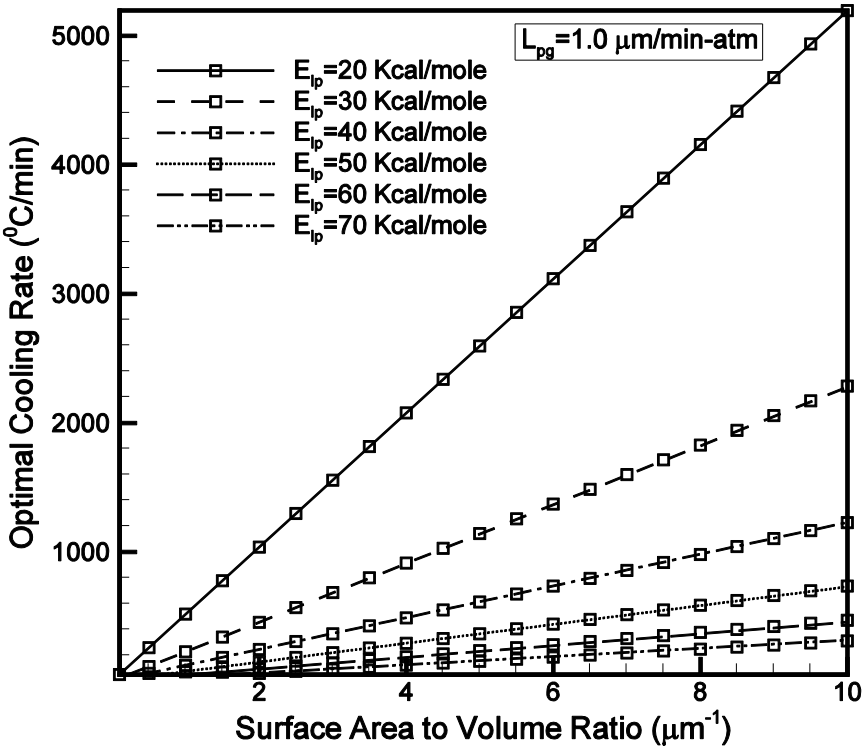

Figure 2.7: Effect of surface area to water volume ratio (SA/WV) on the optimal cooling rate

ratio, the optimal cooling rate increases with the decrease in the activation energy. With the increase in the ratio of SA/WV there is more area available for water to get driven out of the cell. Therefore, the cell requires a lesser time in transporting all the water volume down to ~5% of the initial intracellular water content. As a consequence, the cooling rate increases to meet this criterion.

It is clearly understood that the optimal cooling rate depends on the values of E_{Lp}, $L_{pg,}$ and SA/WV. After knowing the fact that the optimal cooling rate is linearly dependent on the reference membrane permeability and the available surface area to water volume ratio SA/WV, the optimal cooling rate, B_{opt}^{w}, is obtained with setting L_{pg}=1μm/min-atm and SA/WV=1 μm^{-1}. It should be noted here that the actual optimal cooling rate, B_{opt}^{a}, for a cell line is obtained by multiplying the optimal cooling rate with the reference membrane permeability, L_{pg}, and the available surface area to water

volume ratio of that cell. Based on the predicted optimal cooling rate, a correlation is proposed relating the optimal cooling rate and the activation energy of the cell with a goodness of fit 99.9%. The developed correlation is given as,

$$B_{opt}^{w} = 6120.7e^{\left(-0.1574E_{Lp}+1.91\times10^{-3}E_{Lp}^{2}-1.055\times10^{-5}E_{Lp}^{3}\right)} \qquad (9)$$

$$B_{opt}^{a} = B_{opt}^{w} \times (L_{pg})\left(\frac{SA}{WV}\right) \qquad (10)$$

The above correlation is presented in figure 2.8 for a reference membrane permeability of L_{pg} =1μm/atm-min and the ratio of the available surface area for water transport to the initial volume

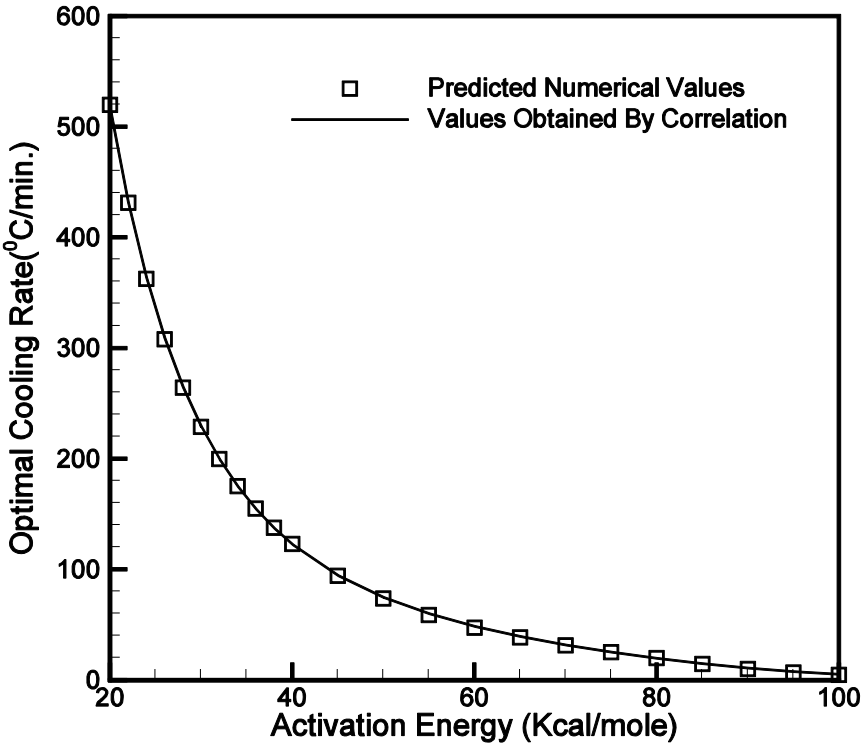

Figure 2.8: Correlation between the Activation Energy and Optimal Cooling Rate, L_{pg} =1μm/atm-min and SA/WV=1 μm^{-1}

of intracellular water SA/WV=1 μm^{-1}. It can be noted that the optimal cooling rates computed numerically (squares) and the optimal cooling rates predicted using the established correlation (solid line) are matching quite well.

The predicted optimal cooling rate by the correlation for certain cell lines is compared with the published experimental/numerical results in Table 1. For example, the optimal cooling rates for Hela cells and diploid oyster sperm are calculated as follows,

A) For Hela cells the input parameters are:

$L_{pg} = 0.05\mu m/(min - atm)$, $E_{lp} = 20.9\ Kcal/mole$, $^{SA}/_{WV} = 0.726\mu m^{-1}$.

With the above input parameters, equation (9) gives $B_{opt}^{w} = 477.12^{0}C/min.$

After putting this value in equation (10) along with the actual values of L_{pg} and $^{SA}/_{WV}$, we get $B_{opt}^{a} = 17.32^{0}C/min.$

B) For, diploid oyster sperm the input parameters are:

$L_{pg} = 0.0019\mu m/(min - atm)$, $E_{lp} = 7.1\ Kcal/mole$, $^{SA}/_{WV} = 16.86\mu m^{-1}$.

With the above input parameters, equation (9) gives $B_{opt}^{w} = 2196.01^{0}C/min.$

After putting this value in equation (10) along with the actual values of L_{pg} and $^{SA}/_{WV}$ gives $B_{opt}^{a} = 70.35^{0}C/min.$

Also, the comparison has been done with the predicted optimal cooling rate by the previously established equation (GOCRE) by Thirumala and Devireddy [46]. It should be noted here that Thirumala and Devireddy have considered -15^0C as the end temperature for the prediction of optimal cooling rate. The percentage error for both the correlations has also been incorporated into the table. It is quite clear that our prediction is more accurate than the prediction obtained with GOCRE. It can also be noticed that the error obtained with the prediction by GOCRE is more when the cell activation energy is less than 20 Kcal/mole (9^{th} column of the table) and the error reduces if the cell activation energy is more than 20 Kcal/mole. But, on the other hand, error obtained with our prediction is very less as compared to the error calculated using GOCRE and the prediction is in close agreement with the published experimental/numerical findings, irrespective of the cell activation energy.

Table 1: Comparison between the optimal cooling rates obtained experimentally and using the present correlation

Cell Type	L_{pg} µm/min-atm	E_{Lp} Kcal/mole	SA/WV	B_{opt} ^{0}C/min (Reported)	B^a_{opt} ^{0}C/min (Predicted)	%Error with predicted B^a_{opt}	B_{opt} ^{0}C/min GOCRE	%Error With GOCRE	Ref.
RBC	2.88	16.34	1.9	5000	4276.617	14.46	2263.55	54.72	[12], [55], [56], [57]
Hela Cells	0.05	20.9	0.726	19.43	17.32	10.75	11.70	39.78	[2]
Equine Sperm	0.02	32.7	7.5	29	28.48	1.7	25.39	12.44	[25]
Fish sperm	0.0093	29	12.12	28	27.59	1.4	23.35	16.60	[52]
Haploid Oyster sperm	0.0017	9.8	22.02	53	58.3	-10	22.13	58.24	[51]
Diploid Oyster sperm	0.0019	7.1	16.86	63	70.35	-11.66	21.95	65.15	[51]
X-helleri Sperm	0.0046	11.97	17.13	89	71.98	19.12	41.14	53.77	[52]
Bovine Sperm	0.036	42.1	12.82	45	50.30	-11.79	46.77	-3.9	[53]
Canine Sperm	0.0029	15.3	15.5	28	37.48	-33.85	19.68	29.71	[54]

*Generic Optimal Cooling Rate Equation (GOCRE) previously established by Thirumala et al. [46]

Figure 2.9 shows the variation of normalised water volume with different cooling rates for E_{Lp}=20 Kcal/mole. The normalised water volume is plotted along y-axis while the sub-cooled temperature is plotted along the x-axis. The cooling rate is taken as 0.5, 1.0, 2.0, and 4.0 times the optimal cooling rate. The optimal cooling rate for this case is 519.6 ^{0}C/min. It should be noted that when the cell is cooled with half of the optimal cooling rate (259.8 ^{0}C/min) the water efflux almost stops at around -15^{0}C and the trapped water is ~1% of the initial osmotically active water volume. The amount of trapped water is calculated as the ratio of trapped water volume at the end temperature of -40 ^{0}C and the initial osmotically active water volume inside the cell, i.e. $(V_{end} - V_b)/(V_0 - V_b)$; V_{end} is cytosol volume at the end temperature of -40^{0}C. With the increase in cooling rate from 259.8 ^{0}C/min to 519.6 ^{0}C/min, 1039.2 ^{0}C/min, and 2078.4 ^{0}C/min the amount of trapped water increases from ~1% to ~5%, ~50%, and

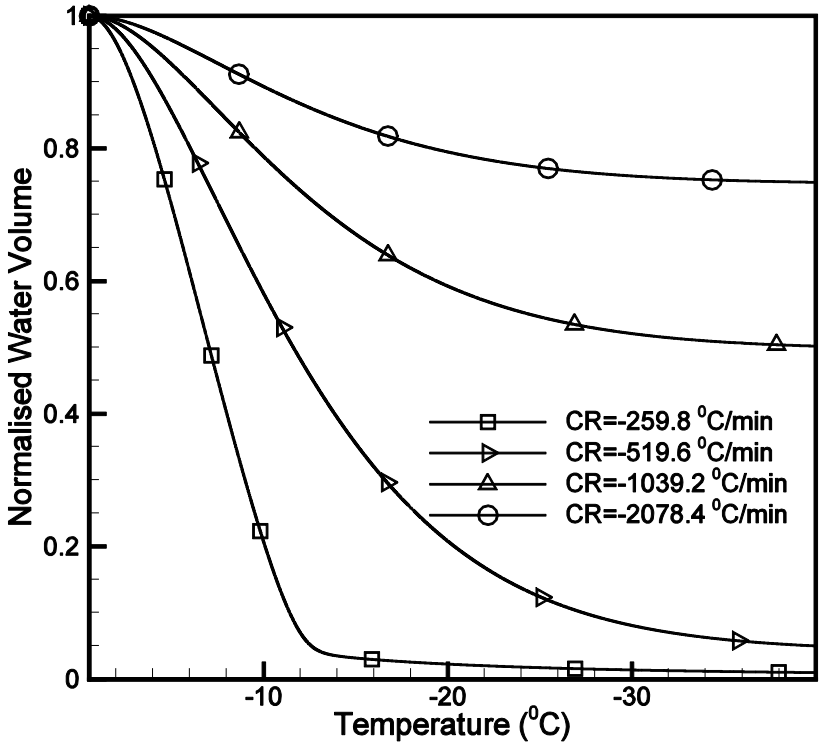

Figure 2.9: Variation of normalised water volume with cooling rate, E_{Lp}=20 Kcal/mole

~75% of the initial osmotically active water volume respectively inside the cell. It is interesting to observe that the amount of normalised water volume reaches its steady value at a temperature of around -15^{0}C, which is much earlier than the previous case, when the cell activation energy is increased to 80 Kcal/mole (see figure 2.10).

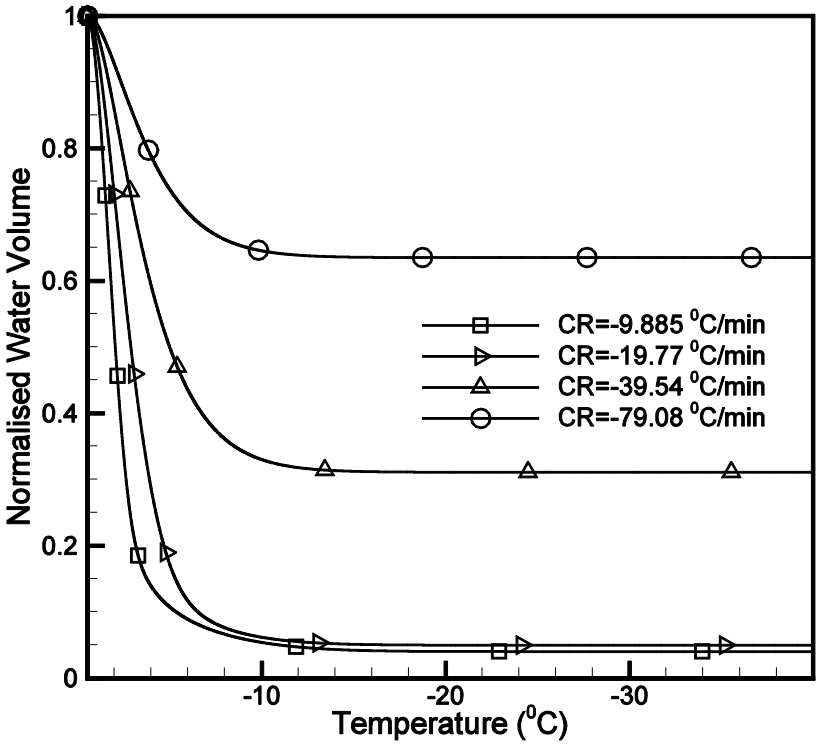

Figure 2.10: Variation of normalised water volume with cooling rate, E_{Lp}=80 Kcal/mole

But, it should be noted that the time required in attaining -15^{0}C temperature is much higher than the time needed by the cell when the activation energy is 20 Kcal/mole. Because, the optimal cooling is equal to 19.77^{0}C/min for the latter case which is almost 1/25th of the previous case (figure 2.9). Also, the amount of trapped water for a cooling rate of 9.885^{0}C/min, 19.77^{0}C/min, 39.54^{0}C/min, and 79.08^{0}C/min becomes ~4%, ~5%, ~31%, and ~64% of the initial osmotically active water volume respectively. It is clear that there is a decrease in the amount of trapped water inside

the cell with the increase in activation energy when the cooling rate is increased by the same factor and is higher than the optimal cooling rate. But, on the other hand, if the cooling rate is decreased by the same factor and is lower than the optimal cooling rate then there is an increase in the amount of trapped water inside the cell when the activation energy increases.

The above discussion suggests that the amount of trapped water depends on the cooling rate as well as on the cell activation energy. An attempt is made to establish a relation between the cooling rate, activation energy, and the normalised trapped water volume at the end of the preservation process, i.e. at an end temperature of -40^0C.

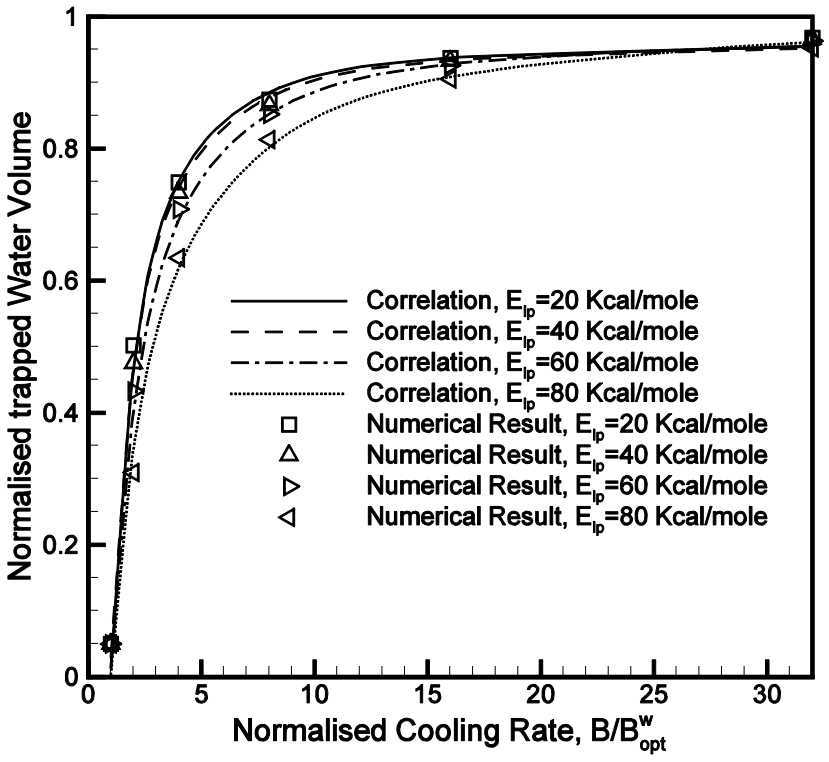

Figure 2.11: Variation of normalised water volume and the normalised cooling rate

Figure 2.11 presents the variation of normalised trapped water volume with the normalised cooling rate. The cooling rate is normalised by the respective optimal cooling rate of the cell. The variation is shown for the activation energies of 20 Kcal/mole, 40 Kcal/mole, 60 Kcal/mole, and 80 Kcal/mole. The data is obtained by varying the cooling rate with a rate equals to 1, 2, 4, 8, 16, and 32 times the optimal cooling rate. It can be noticed that the amount of normalised trapped water volume increases with a decrease in the activation energy for a given normalised cooling rate. Also, the difference in the normalised trapped water volume increases initially and later on decreases with the increase in normalised trapped water volume. It is worth noting that the values of normalised trapped water volume almost collapse into a single value at a normalised cooling rate of 32.

Based on the simulated data for normalised trapped water volume, a correlation is proposed which is given as,

$$\left.(V_{end} - V_b)\right/(V_0 - V_b) = A^w + B^w \times e^{(-C^w \times B^{0.3})} \qquad (11)$$

Where,

$$A^w = 9.72 \times 10^{-1} - 1.055 \times 10^{-3} E_{lp} + 1.625 \times 10^{-5} E_{lp}^2$$

$$B^w = -2.215 \times 10^{1} + 9.67 \times 10^{-2} E_{lp} + 1.2 \times 10^{-3} E_{lp}^2$$

$$C^w = 2.959 \times 10^{0} + 8.61 \times 10^{-3} E_{lp} - 2.7 \times 10^{-4} E_{lp}^2$$

The above correlation is obtained with a goodness of fit 99.8%. This correlation is valid for 20 Kcal/mole $\leq E_{Lp} \leq$ 80 Kcal/mole.

2.5 CONCLUSION

The effect of end temperature on the optimal cooling rate has been discussed in this study and found that the combination of 5% trapped water and an end temperature of -40^0C is more significant for predicting the optimal cooling rate of cryopreserving a cell. The effect of E_{Lp}, SA/WV, and L_{pg} on optimal cooling rate has also been studied and found out that optimal cooling rate is linearly dependent on L_{pg} and SA/WV. However, the optimal cooling rate varies non-linearly with E_{Lp}. Based on the predicted optimal cooling rate, a correlation formula has been established with a goodness of fit 99.9%. Using this correlation the optimal cooling rate can be predicted for various cell lines provided the cell parameters are know a priori and this will help in preservation of cells for longer period of time with maximum survivability.

CHAPTER 3

EFFECT OF CRYOPROTECTANT ON THE OPTIMAL COOLING RATE

3.1 INTRODUCTION

Cell experiences freezing injury by two distinct mechanisms. The first one comes under mechanical damage as the shape of the cell is distorted by ice crystals, the other one is damage caused by chemical and osmotic effects of concentrated solutes in the residual unfrozen water. This is known as "solution effects" injury. To overcome these freezing injuries cryoprotectants (CPAs) are being added to the system as they dissolve in water and lower the freezing point of water. Hence cryoprotectants can be defined as the chemicals that protect living things from being injured by freezing during exposure to subzero temperature or in other words cryoprotection can be described as a process of replacement of water molecules with other molecules that do not freeze when exposed to low temperature. The most commonly used CPAs for cell preservation are glycerol and DMSO. Depression of freezing point, with the addition of CPA, is a function of CPA concentration which in turn influences the optimal cooling rate. Therefore, it is extremely essential to study the effect of CPA on the optimal cooling rate.

In this chapter, the effect of DMSO concentration on the optimal cooling rate has been studied and a correlation between optimal cooling rate, cell geometry and biophysical parameters, and DMSO concentration is established. The DMSO concentration is varied between 0.1M and 1.3M.

So considering DMSO as the cryoprotectant, volumetric changes of the cell has been studied by varying the initial concentration (c_{gi}) of DMSO from 0.1M to 1.3M. The alteration in the salt concentration as well as water volume has also been analyzed in the presence of DMSO and the results have been presented in the following sections.

3.2 GOVERNING EQUATION

The modified water transport model [18] to incorporate the presence of CPA is considered and the equation is given as, (as mentioned in chapter 1, Eq. 7),

$$\frac{dV}{dT} = -\frac{L_p A_c RT}{B v_w}\left[ln\frac{(V_0 - V_b - n_g v_g)/v_w}{(V_0 - V_b - n_g v_g)/v_w + (\varphi_s n_s + n_g)} - \frac{\Delta H_f v_w \rho}{R}\left(\frac{1}{T_R} - \frac{1}{T}\right)\right] \qquad (7)$$

And L_p is given as below (as mentioned in chapter 1, Eq. 8),

$$L_p = L_{pg}\, exp\left[-\frac{E_{Lp}}{R}\left(\frac{1}{T} - \frac{1}{T_R}\right)\right] \qquad (8)$$

The new parameters introduced in the equation are n_g and v_g where, n_g is the number of moles of cryoprotectant in the cell (DMSO in this study) and v_g is the partial molar volume of the cryoprotectant. All the other parameters are the same as explained in chapter 1.

3.3 NUMERICAL APPROACH

The above mentioned equation is solved using fourth order Runge-Kutta method to predict the optimal cooling rate. In the equations, the important input parameters are: reference membrane permeability L_{pg}, activation energy E_{Lp}, available surface area to water volume ratio SA/WV, and the initial concentration of DMSO. As observed in chapter 2, the optimal cooling rate is linearly dependent on L_{pg} and SA/WV, therefore, the optimal cooling rate is obtained with keeping L_{pg}=1 μm/min-atm and SA/WV=10 μm^{-1}. The other parameters are varied in the range of 20 Kcal/mole ≤ E_{Lp} ≤ 80 Kcal/mole and 0.1M ≤ c_{gi} ≤ 1.3M. The salt concentration is taken equal to 0.142M.

3.4 RESULTS & DISCUSSION

The water gets transported across the cell membrane when it is subjected to a cooling condition. As a result, the concentration of solute as well as the concentration of CPA increases with the efflux of water and as described earlier in chapter 1 optimal cooling rate has a great impact on the volume of water efflux and the survival rate of a cell. So, in order to get detailed information, simulations have been carried out by considering the parameters like concentration of CPA, concentration of salt (NaCl) and normalised water volume. As mentioned earlier, all the cell shrinkage data is obtained with an assumption of 5% of the initial amount of intracellular trapped water inside the cell and the end temperature is considered to be -40 ^{0}C for rest of the study and it should be noted that the values are obtained with the following input parameters: L_{pg} =1μm/min-atm, SA/WV= 10 μm^{-1} and V_b= 0.6 V_0. The simulations have been carried out with activation energy varying between 20 Kcal/mole and 70 Kcal/mole, the initial concentration of DMSO varying between 0.1M and 1.3M. The initial condition of the system is taken as the depressed freezing point of water because of the given initial concentration of DMSO.

Variation of DMSO concentration

For this case the CPA is considered to be DMSO and to understand its effect on optimal cooling rate the DMSO concentration is plotted with the temperature with the cell activation energies of 20 Kcal/mole and 40 Kcal/mole. Here, c_{gi} refers to the initial concentration of DMSO ranging from 0.1 M to 1.3 M.

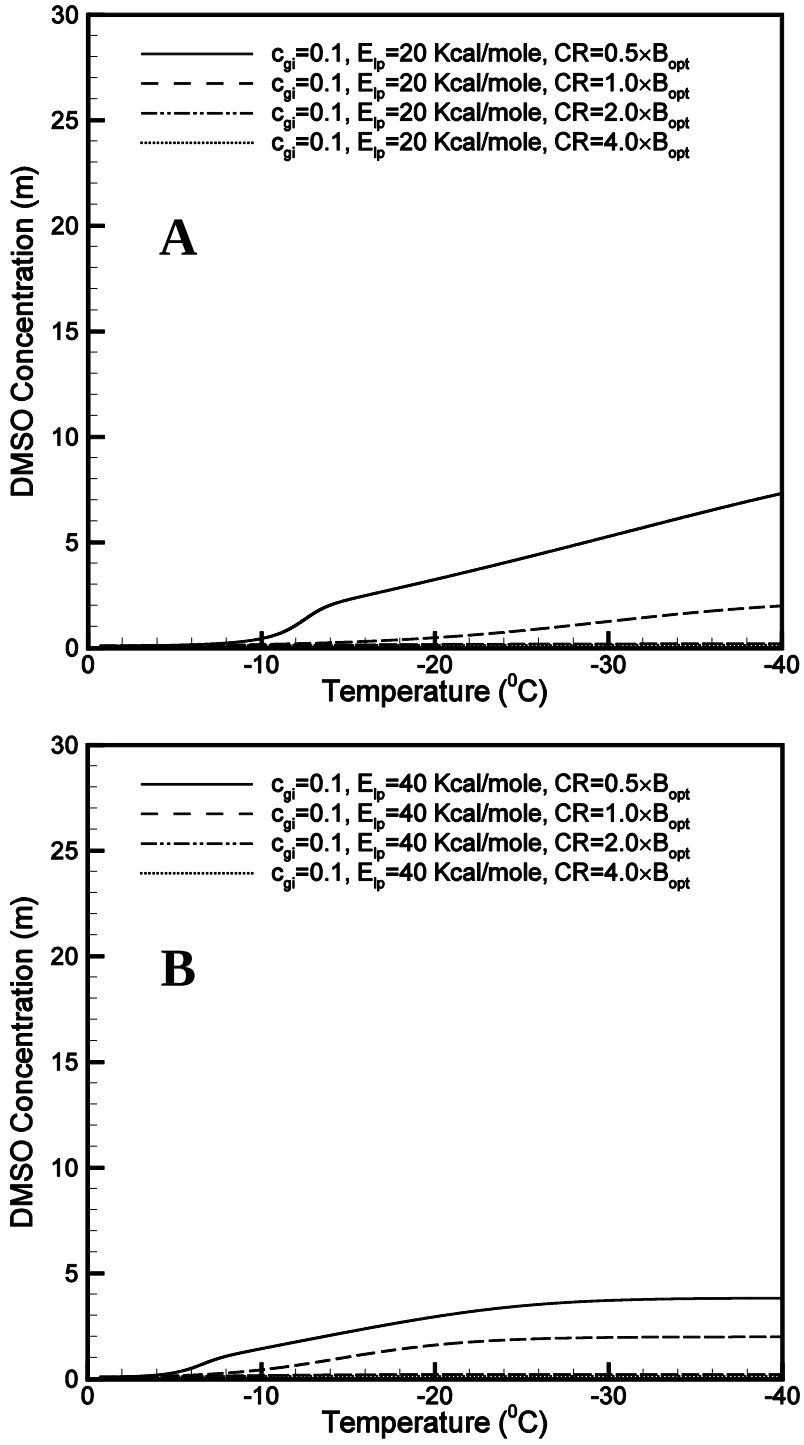

Figure 3.1: Variation of DMSO concentration with temperature at c_{gi} = 0.1M, E_{Lp} = 20 Kcal/mole (A) and E_{Lp} = 40 Kcal/mole (B)

Figure 3.1 shows the variation of DMSO concentration for different cooling rates. Figure 3.1 A corresponds to the variation for E_{Lp}= 20 Kcal/mole while figure 3.2 B is for E_{Lp}= 40 Kcal/mole. In the figure, c_{gi} is the initial concentration of DMSO inside the cell, CR is the cooling rate. Though the initial concentration of DMSO (c_{gi}) is same for both the cases but the range of final concentrations vary from 0.1 to 7.2m for E_{Lp}= 20 Kcal/mole (figure 3.1 A) and 0.1 to 4M for E_{Lp}= 40 Kcal/mole (figure 3.1 B) when the cooling rate CR is half of the optimal cooling rate. It should be noted that there is a sharp increase in the DMSO concentration in the beginning of the process followed by almost a linear increase for a lower value of E_{Lp}=20 Kcal/mole. However, this variation is entirely different when E_{Lp} value is increased to 40 Kcal/mole. Initially, the trend is almost similar but later on the DMSO concentration assumes a steady value which shows that water efflux has stopped and there is no change of cytosol volume. It is clear that for higher cooling rates, e.g. CR= 2 × B_{opt} and CR= 4 × B_{opt}, there is hardly any loss of water from the cytosol. Therefore, the DMSO concentration for these cases does not vary much as reflected in figure 3.1. Also, it should be noted that for a lower cooling rate, initially the water loss is more for the cell with higher activation energy. It can be noticed that end value of the concentration of DMSO is same when the cells with different activation energies are cooled with the optimal cooling rate B_{opt}. This value is equal to 2m. This is quite obvious because, as per the definition of optimal cooling rate, 5% of the initial intracellular water should be trapped inside the cytosol at an end temperature of -40^{0}C. The end concentration of DMSO varies between 0.1m-4.0m and 0.1m-7m for E_{Lp} values of 40Kcal/mole and 20 Kcal/mole respectively.

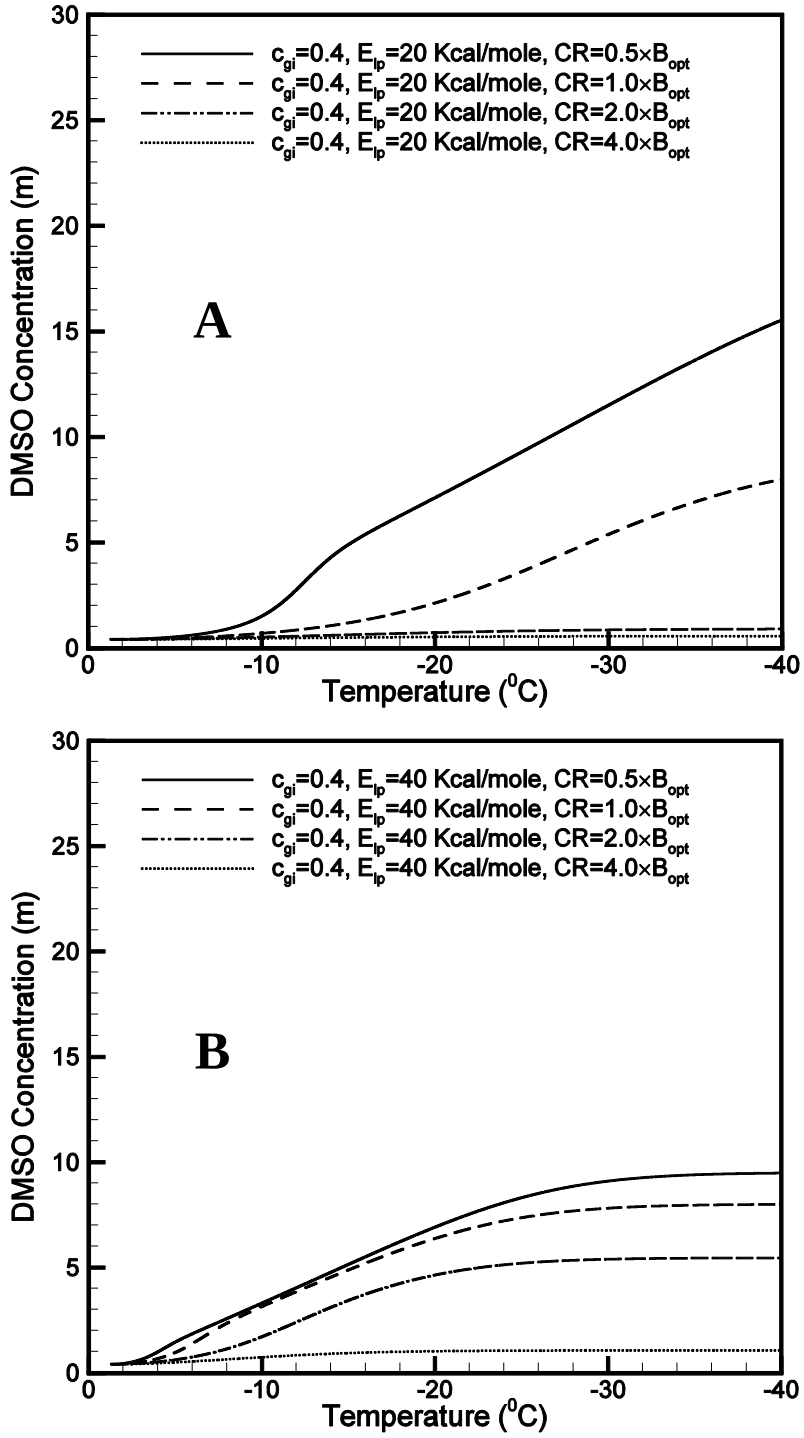

Figure 3.2: Variation of DMSO concentration with temperature at c_{gi} = 0.4M, E_{Lp} = 20 Kcal/mole (A) and E_{Lp} = 40 Kcal/mole (B)

Almost similar trends have been observed in figure 3.2 when the initial concentration of DMSO is increased to 0.4M. But, the end concentration of DMSO is almost double that of the case with c_{gi}= 0.1M when the cells are cooled with half of the optimal cooling rate. The range of variation of c_g at the end becomes 15m and 9m for cells with low and high activation energies respectively. Therefore, it is suggested that with an increase in c_{gi} from 0.1M to 0.4M the range of cooling rate decreases which can give maximum survivability of the cells. Although, for higher cooling rate i.e. CR= 4 $\times B_{opt}$, the water loss is almost negligible for both the cases but, there is significant water loss when the cell with higher activation energy is cooled with a rate which is twice the optimal cooling rate. This effect is more pronounced when the initial concentration of DMSO is increased further to 0.7M (see figure 3.3 B). Now, even at the highest cooling rate i.e. CR= 4 $\times B_{opt}$, there is a significant water loss which results in the increase of DMSO concentration with time. Also, it can be noticed that with increase in the initial concentration of DMSO the increase in water loss is more when the cell is cooled with a higher cooling rate. It is noteworthy that the cell dehydration is almost similar up to -15^{0}C irrespective of the cooling rate for cells with higher value of activation energy. It is interesting to observe that the range of end concentration of DMSO is increased from 15m to 18m for cell with low activation energy suggesting that the range of cooling rate for maximum survivability gets further decreased. But, on the other hand, this range decreased from 9m to 5m for cells with high activation energy (see figure 3.3 B) thereby increasing the range of cooling rate which can give maximum survivability.

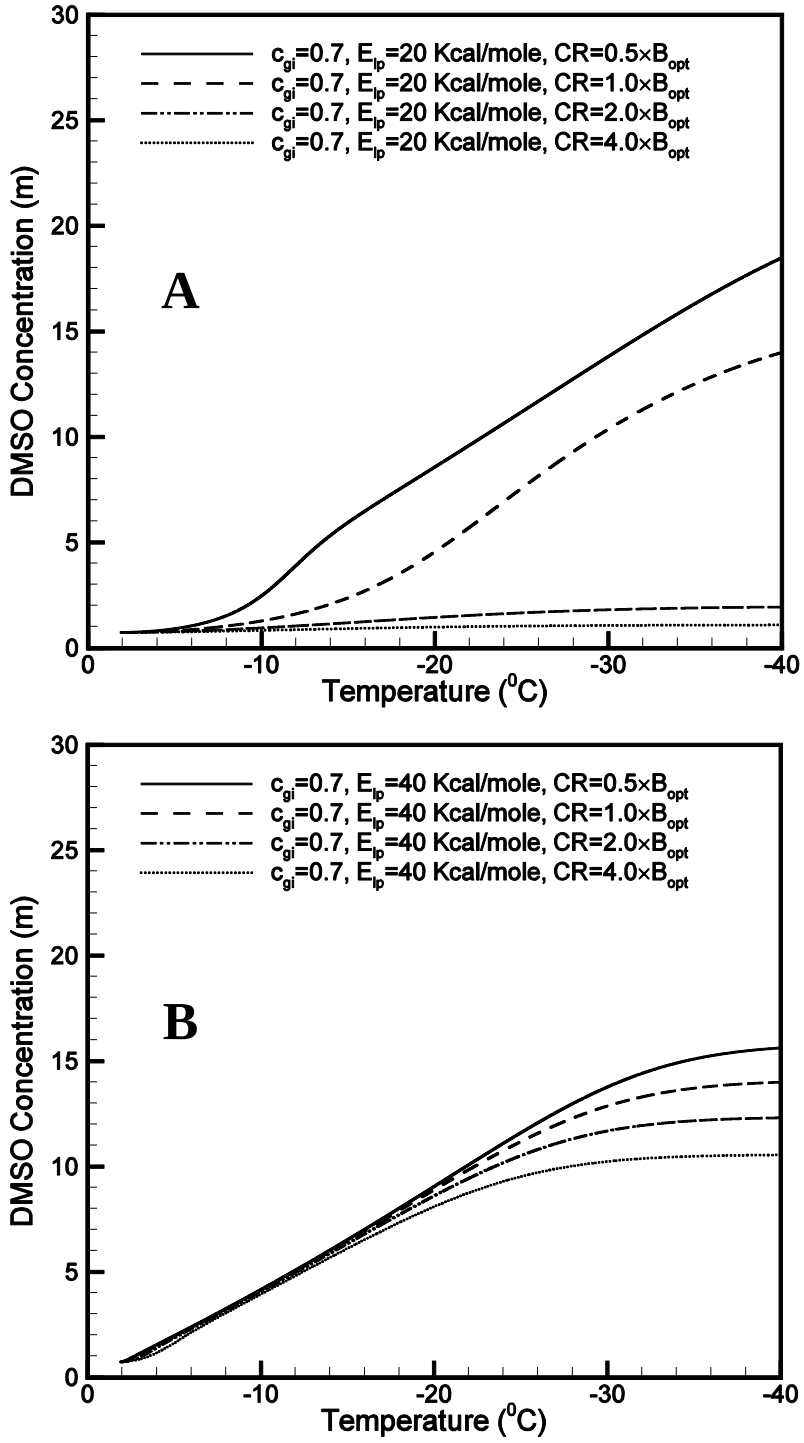

Figure 3.3: Variation of DMSO concentration with temperature at c_{gi} = 0.7M, E_{Lp} = 20 Kcal/mole (A) and E_{Lp} = 40 Kcal/mole (B)

With further increase in the initial concentration of DMSO from 0.7M to 1.0M the range of end concentration changed to 19m and 5m for cells with low and high activation energies. Although, the range is 5m for figure 3.4 B, the end concentration value varies between 16.8m and 21.8m showing that with increase in initial concentration of DMSO the end concentration increases. Also, the cell dehydration is almost similar till -22^0C irrespective of the cooling rate. Now, for this case, there is a significant water loss at higher cooling rate from the cytosol even when the cell activation energy is low (see figure 3.4 A). Although, the range of end concentration is high (i.e. 19m) but the difference between the value of end concentration obtained with optimal cooling rate and the CR= $4 \times B_{opt}$ is less compared to the previous case of c_{gi}=0.7M.

Figure 3.5 shows the variation of DMSO concentration with different cooling rates for cells having low (20 Kcal/mole) and high (40 Kcal/mole) activation energies when c_{gi}=1.3M. For this case, the trend is entirely different. Now, the water transportation across the cell membrane is influenced neither by the cooling rates nor by the activation energies. Although, there is little variation at the end but most of the time it remains almost similar. So, it can be concluded that with an increase in the initial concentration of DMSO the range of cooling rates, for which the cell survivability is higher, increases.

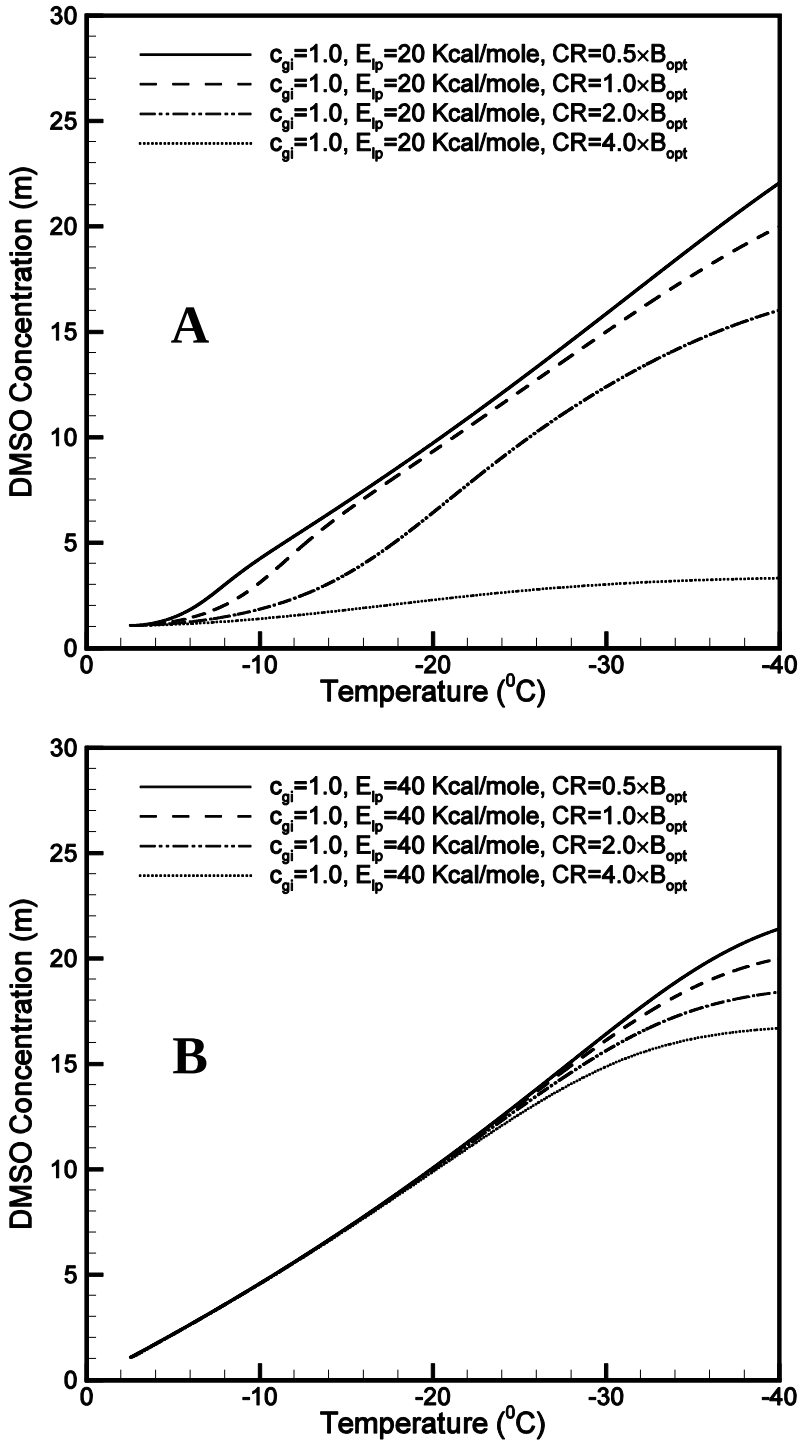

Figure 3.4: Variation of DMSO concentration with temperature at c_{gi} = 1.0M, E_{Lp} = 20 Kcal/mole (A) and E_{Lp} = 40 Kcal/mole (B)

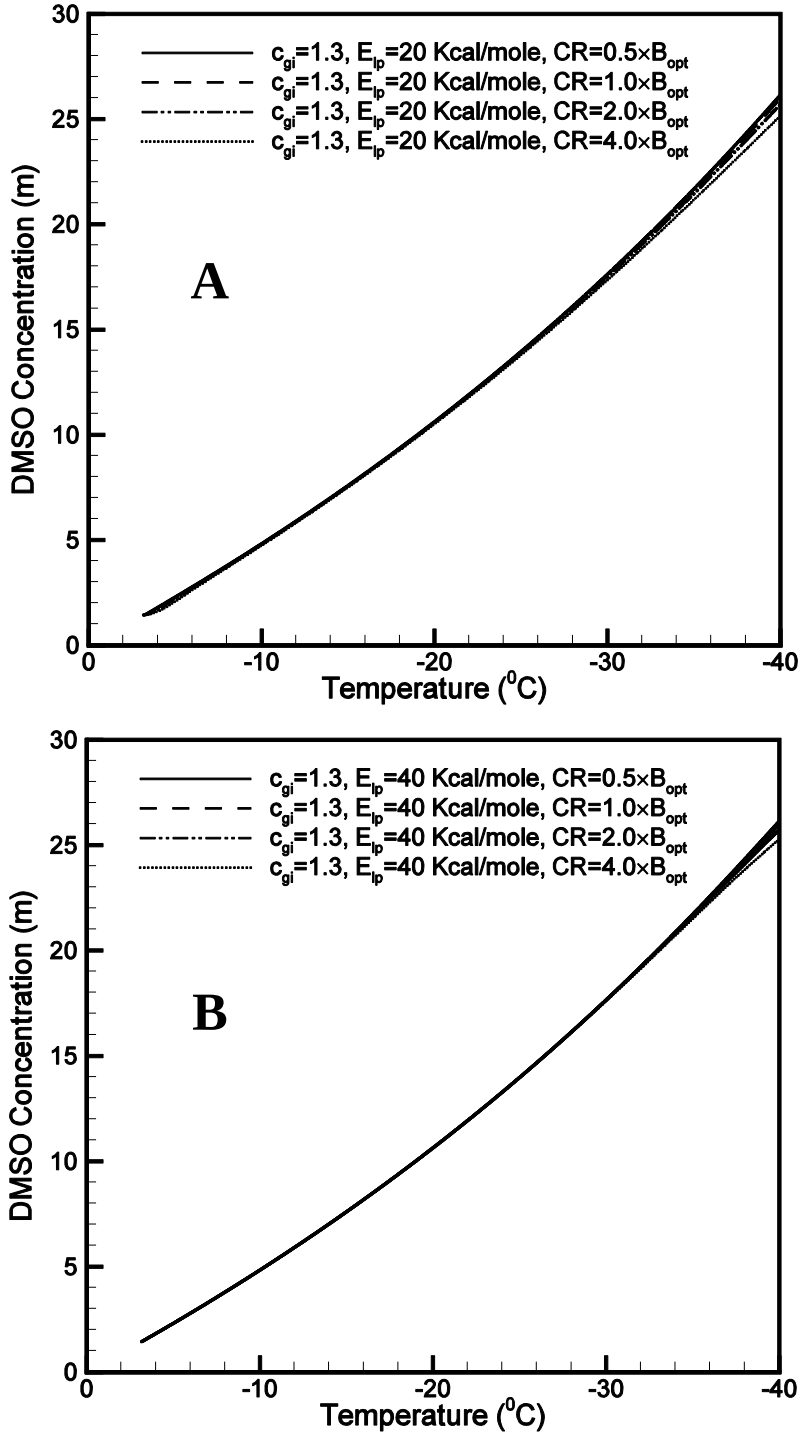

Figure 3.5: Variation of DMSO concentration with temperature at c_{gi} = 1.3M, E_{Lp} = 20 Kcal/mole (A) and E_{Lp} = 40 Kcal/mole (B)

Variation of salt concentration

Along with water and CPA, salt concentration also alters during the preservation process. Hence, it is equally important to study the concentration of salt within a cell when it is subjected to freezing. As salt concentration causes damage to the cell [11], its variation has been studied in detail.

It has already been stated that slow cooling causes dehydration, as a result the solute concentration within the cell increases and figure 3.6 completely depicts this phenomenon. It can be noticed that the difference in initial and final salt concentrations is much higher at CR = 0.5 × B_{opt} (0.142m to 10.4m (A), 0.142m to 5.4m (B)) than that of CR = 4 × B_{opt}(almost no change for both the cases). This is because, at slow cooling rate, more amount of water gets driven out of the cell and hence the salt concentration increases rapidly and with the increase in cooling rate the intracellular water does not get enough time to get transported across the plasma membrane. Therefore, there is almost no significant change in the salt concentration (for both the figures 3.6 A and B). Also, it should be noted that the final salt concentration is higher for cells having low activation energy and cooled with slow cooling rate i.e. CR = 0.5× B_{opt}. However, this trend is entirely opposite when the cells are cooled with a cooling rate higher than the optimal cooling rate B_{opt}. Now, the final concentration of salt is more for cells with higher activation energy. And, as expected, the final salt concentration is same when the cell is cooled with optimal cooling rate. But, the attainment of the final concentration (2.8m) from the initial concentration (0.142m) is different for both the cases which indicate that the cells have dehydrated differently.

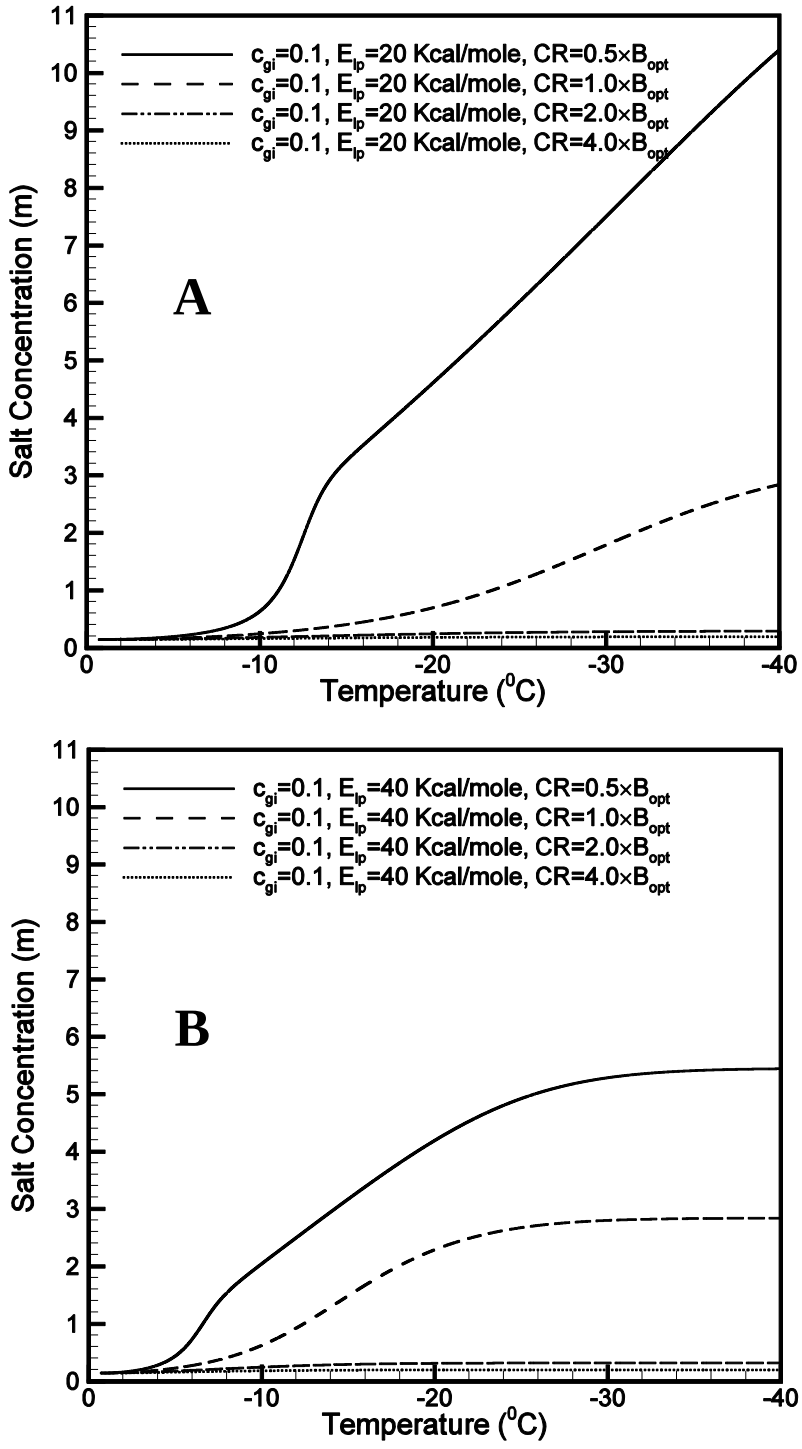

Figure 3.6: Variation of salt concentration with temperature at c_{gi} = 0.1M, E_{Lp} = 20 Kcal/mole (A) and E_{Lp} = 40 Kcal/mole (B)

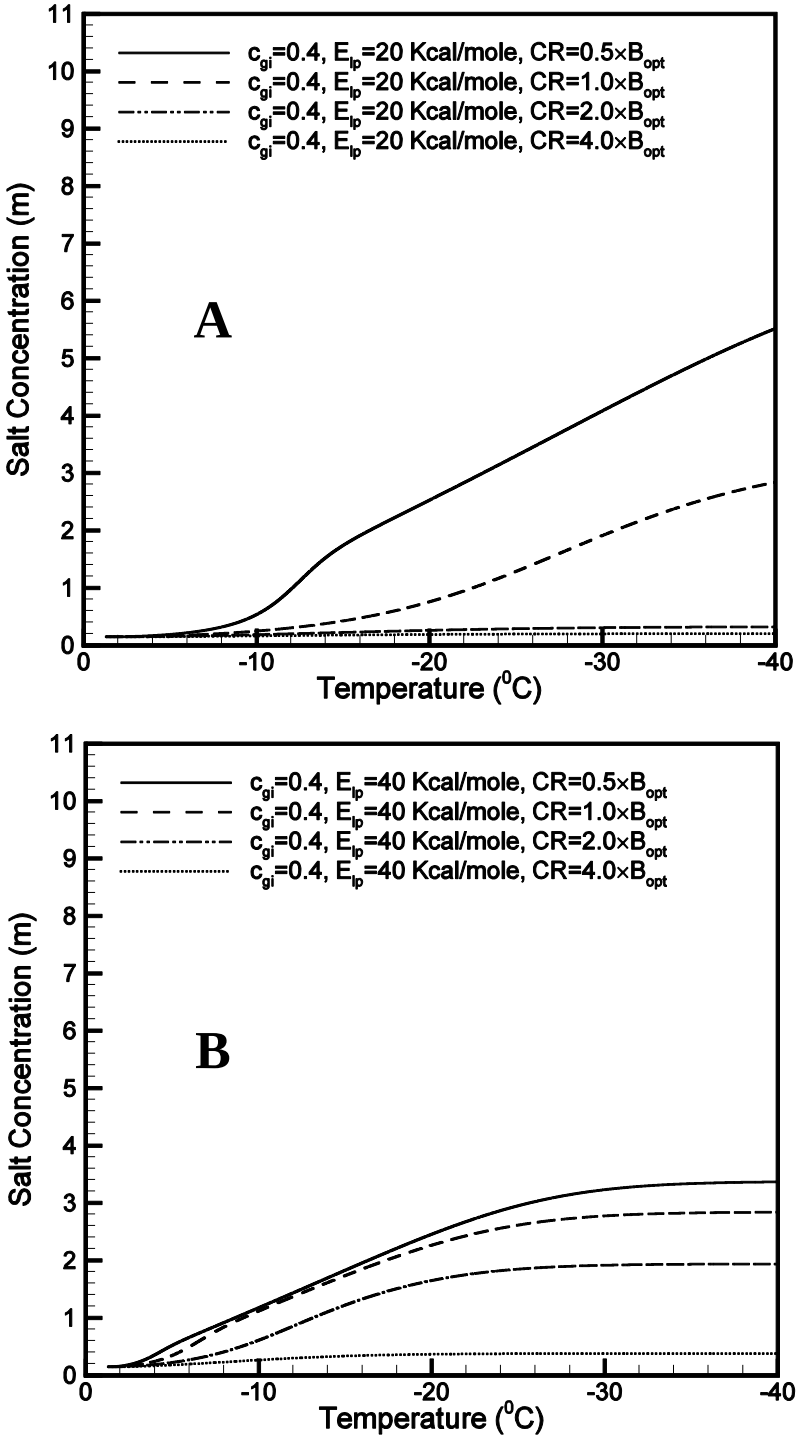

Figure 3.7: Variation of salt concentration with temperature at c_{gi} = 0.4M, E_{Lp} = 20 Kcal/mole (A) and E_{Lp} = 40 Kcal/mole (B)

It is interesting to observe that with increase in the initial DMSO concentration the final salt concentration decreases (see figure 3.7) when the cells are cooled with a cooling rate lower than the optimal cooling rate. On the other hand, the final concentration of salt increases when the cells are cooled with a cooling rate higher than the optimal cooling rate. But, most important thing is that when the cells are cooled with a cooling rate equal to the optimal cooling rate, the final salt concentration does not change. It remained at its earlier value of 2.8m when the initial DMSO concentration was 0.1M. However, this is not the case with final DMSO concentration (see figures 3.1 and 3.2) even when the cells are cooled with optimal cooling rate. This is quite obvious; the solute concentration has been defined as the ratio of number of moles of the solute to the water volume inside the cell. The final salt concentration at optimal cooling rate is same because water volume is same at the end and, also, initial salt concentration is fixed at 0.142m for all the cases. Although, the end water volume remains same for all the cases when the cells are cooled with optimal cooling rate, the final concentration of DMSO changed because of the change in its initial concentration. With the further increase in initial DMSO concentration to 0.7M the final salt concentration further decreases, when the cells are cooled with the cooling rate lower than the optimal cooling rate (see figure 3.8). There is a significant change in final concentration for the cells having high activation energy; on the other hand, cells cooled with higher cooling rate do not show any appreciable increase in the final concentration.

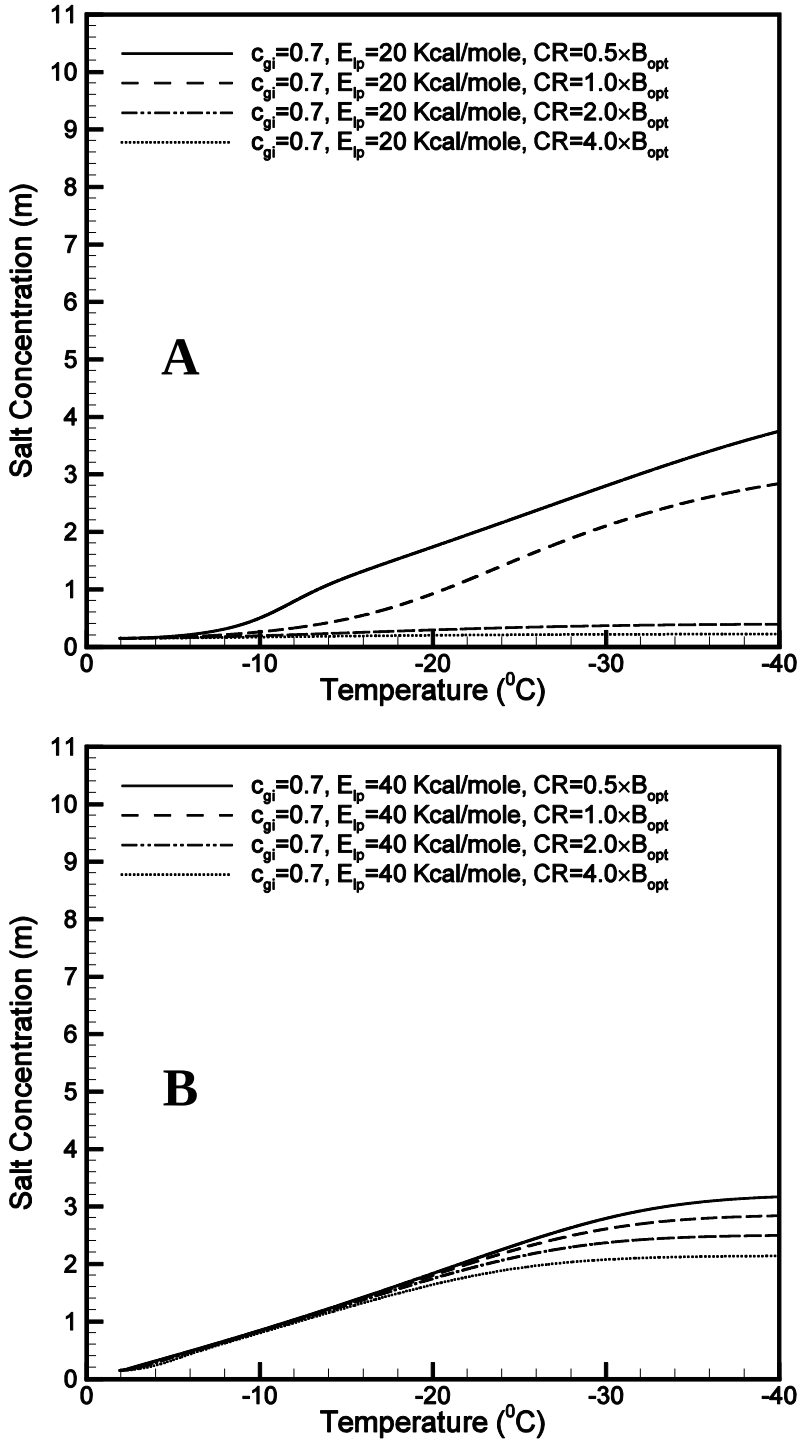

Figure 3.8: Variation of salt concentration with temperature

at c_{gi} = 0.7M, E_{Lp} = 20 Kcal/mole (A) and E_{Lp} = 40 Kcal/mole (B)

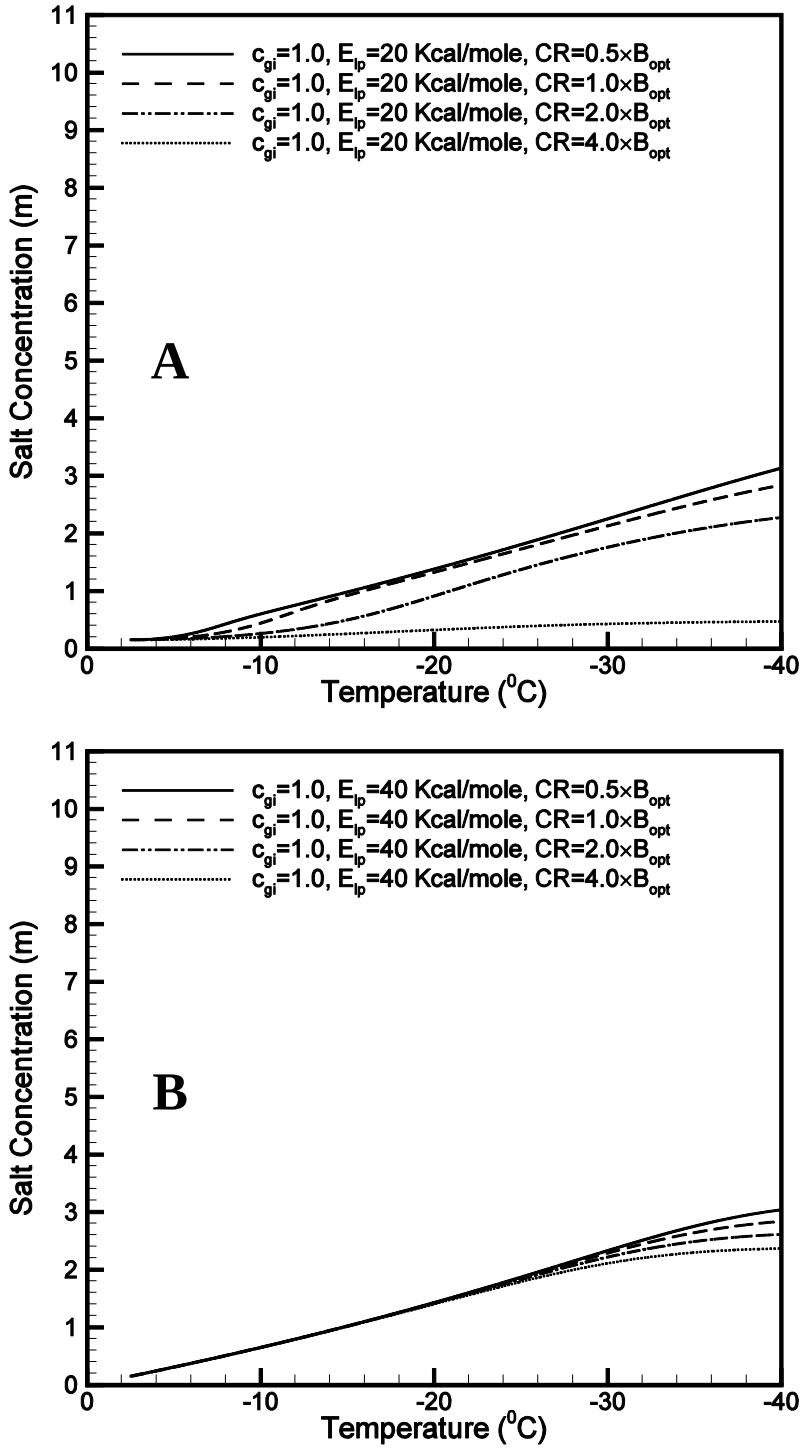

Figure 3.9: Variation of salt concentration with temperature at c_{gi} = 1.0M, E_{Lp} = 20 Kcal/mole (A) and E_{Lp} = 40 Kcal/mole (B)

Figure 3.9 shows the variation of salt concentration when the initial DMSO concentration is increased to 1.0M. Now, there is a significant increase in the final concentration of salt when the cooling rate is twice the optimal cooling rate and activation energy E_{Lp}=20 Kcal/mole. However, when the cells are cooled with a cooling rate CR= 4× B_{opt}, the final salt concentration changes from 0.2m to 0.42m with the increase in initial DMSO concentration from 0.7M to 1.0M. But, on the other hand, the final salt concentration of the cells having higher activation energy converges towards the value of final salt concentration when the cells are cooled with optimal cooling rate, i.e. 2.8m. Like the variation of DMSO concentration, the variation of salt concentration is almost same till -22^{0}C irrespective of the cooling rate (see figure 3.4 B and figure 3.9 B).

Similar trend, as that of DMSO concentration, is noticed when the initial DMSO concentration is increased to 1.3M (see figure 3.10). For this case also, the trend is entirely different; all the curves collapsed into a single one corresponding to the curve for optimal cooling rate. As observed during variation of DMSO concentration, there is no influence of cooling rate and activation energy on the water transportation across the cell membrane. Although, there is little variation at the end but most of the time it remains almost similar.

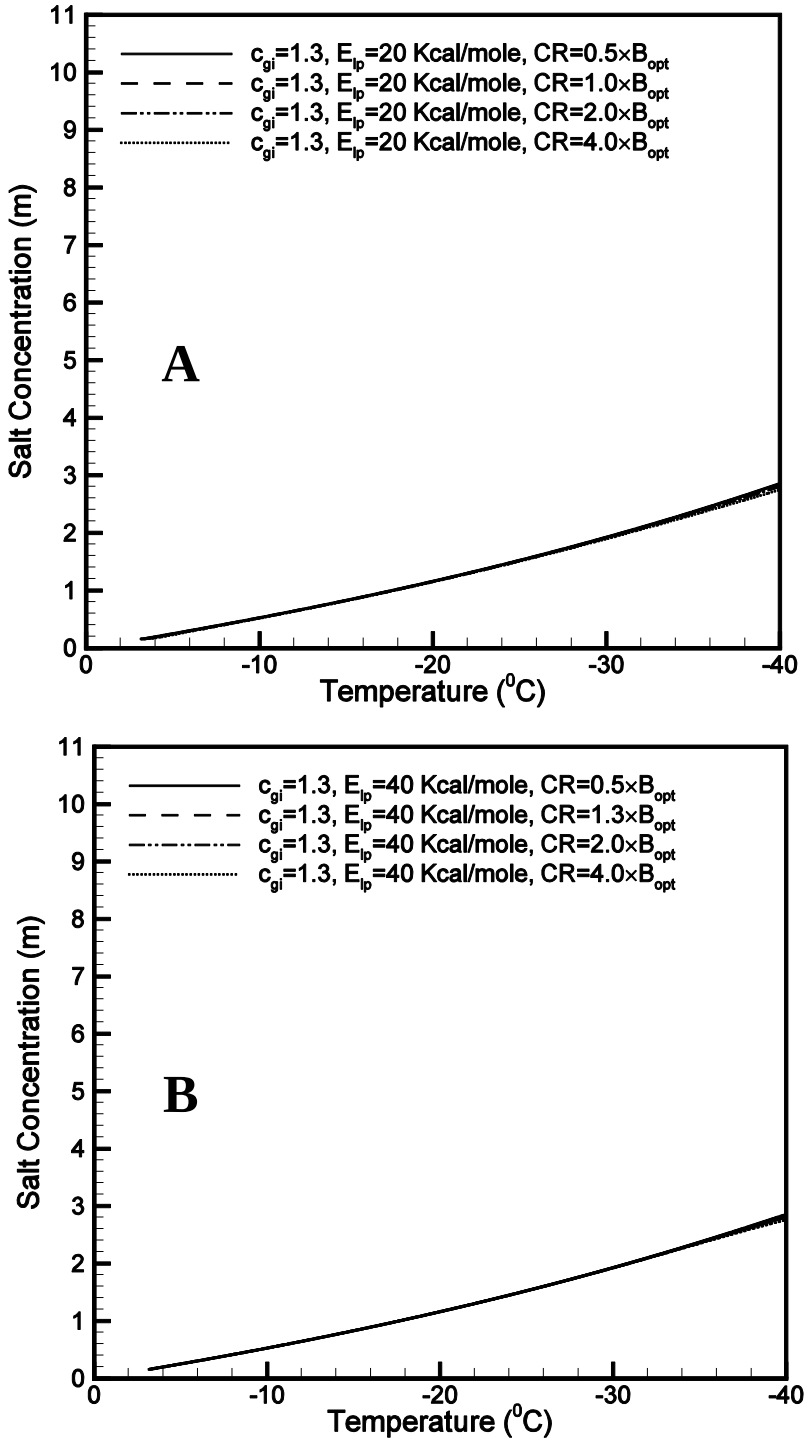

Figure 3.10: Variation of salt concentration with temperature at c_{gi} = 1.3M, E_{Lp} = 20 Kcal/mole (A) and E_{Lp} = 40 Kcal/mole (B)

Variation of normalised water volume

The simulation has been carried out to study the volumetric changes of cell when subjected to freezing condition in the presence of CPA. For this case also, the initial concentration of DMSO is varied from 0.1M to 1.3M for two different values of activation energies (20 Kcal/mole and 40 Kcal/mole) and the results are presented in the following section.

It is well known that water transportation will be more in case of slow cooling rate and with the increase in cooling rate it slows down. Similar behaviour is observed in figure 3.11 which shows the variation of normalised water volume with temperature for cell activation energies of 20 Kcal/mole and 40 Kcal/mole with an initial concentration of DMSO equals to 0.1M. The normalised water volume is obtained by dividing the water volume with the isotonic initial content of water. The change in water volume is more in the case of lower cooling rate (CR=0.5× B_{opt}) and as the cooling rate increases, the cytosol water does not get sufficient time to get driven out of the cell. It should be noted that when the cell with higher activation energy is cooled with slow cooling rate the variation in normalised water volume closely follows the trend when the cell is cooled with optimal cooling rate. But, the variation is different for cells with low activation energy. Also, the change in water volume almost stopped after -20^{0}C for the cells with high activation energy, irrespective of the cooling rates. However, the change in water volume continues till -36^{0}C for the cells with low activation energy.

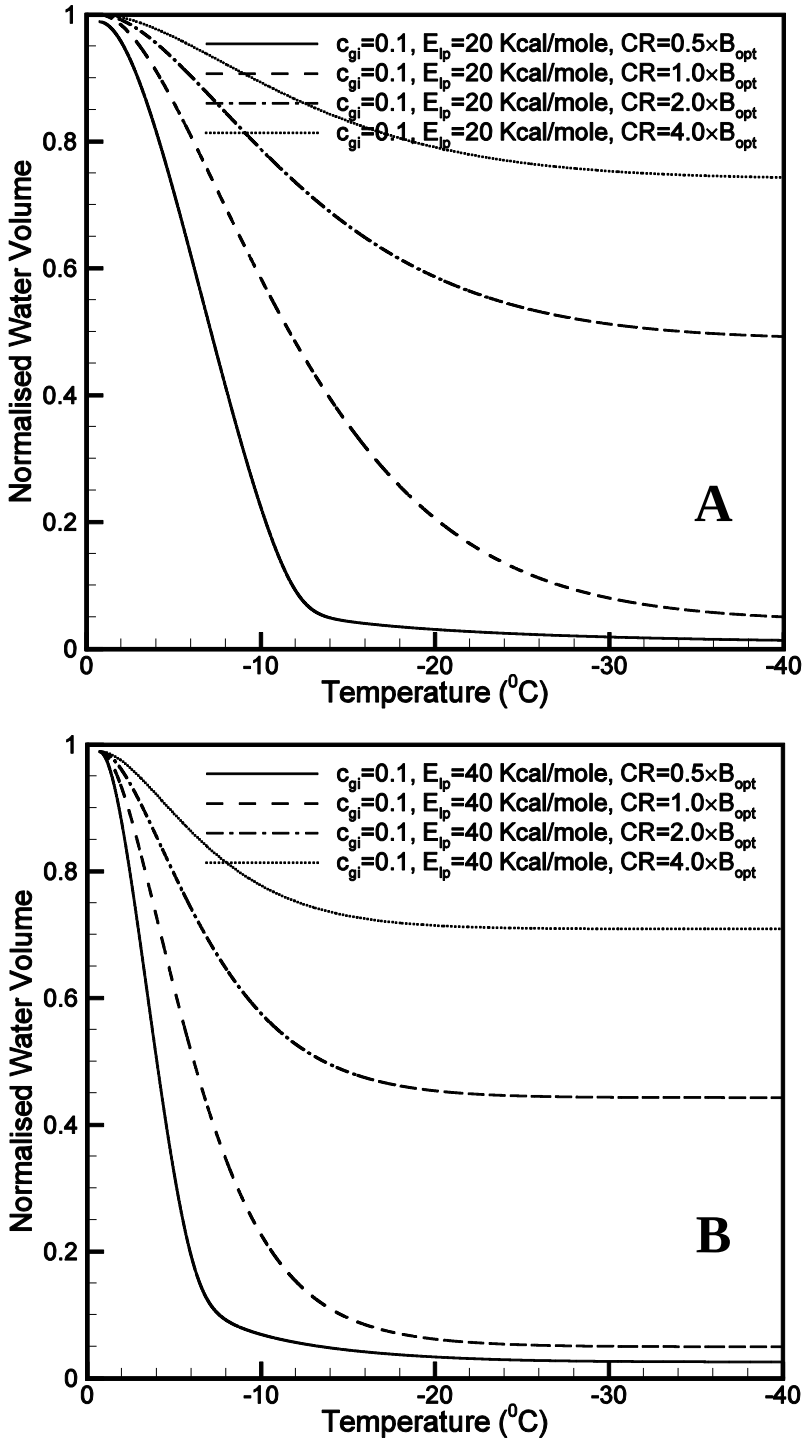

Figure 3.11: Variation of normalised water volume with temperature at $c_{gi} = 0.1M, E_{Lp}$ = 20 Kcal/mole (A) and E_{Lp}= 40 Kcal/mole (B)

Freezing point depression which occurs due to addition of CPA is very well observed in figure 3.12. Here, the normalised water volume has been plotted against temperature with an increased value of c_{gi} (0.4M) and due to the addition of CPA it can be seen that the initial temperature has been shifted to -1.3^{0}C which is -0.7^{0}C for the previous case (figure 3.11). It should be noted that the initial temperature of the cell is assumed to be equal to the equilibrium freezing point of the cytosolic water. Now, the cell response, when cooled at CR = 0.5× B_{opt}, is almost similar to the cell response when it is cooled with optimal cooling rate for the cell with high activation energy (see figure 3.12 B). Therefore, it is suggested that cell injury due to solution effect can be minimised when DMSO is added to the cell with 0.4M concentration. Also, the range of final normalised water volume varied from 0.05 to 0.75 for case A whereas it is varying from 0.05 to 0.55 for case B. With the further increase in the initial DMSO concentration to 0.7M (figure 3.13), the depression in freezing point is increased; now, the initial temperature is changed to -1.9^{0}C. It is interesting to observe that there is a distinct change in water volume for each of the cooling rates at E_{Lp}= 20 Kcal/mole (A) and four different curves are obtained for normalised water volume. But, at E_{Lp}= 40 Kcal/mole (B) the variation is almost negligible. The curves are hardly being distinguished from each other even though the cooling rate is varied between CR = 0.5× B_{opt} and CR = 4.0× B_{opt}. This is in close agreement with the previous conclusion (figure 3.3 B) that the range of cooling rate, for which the cell survivability is maximised, increases for cells with high activation energy with initial 0.7M DMSO concentration.

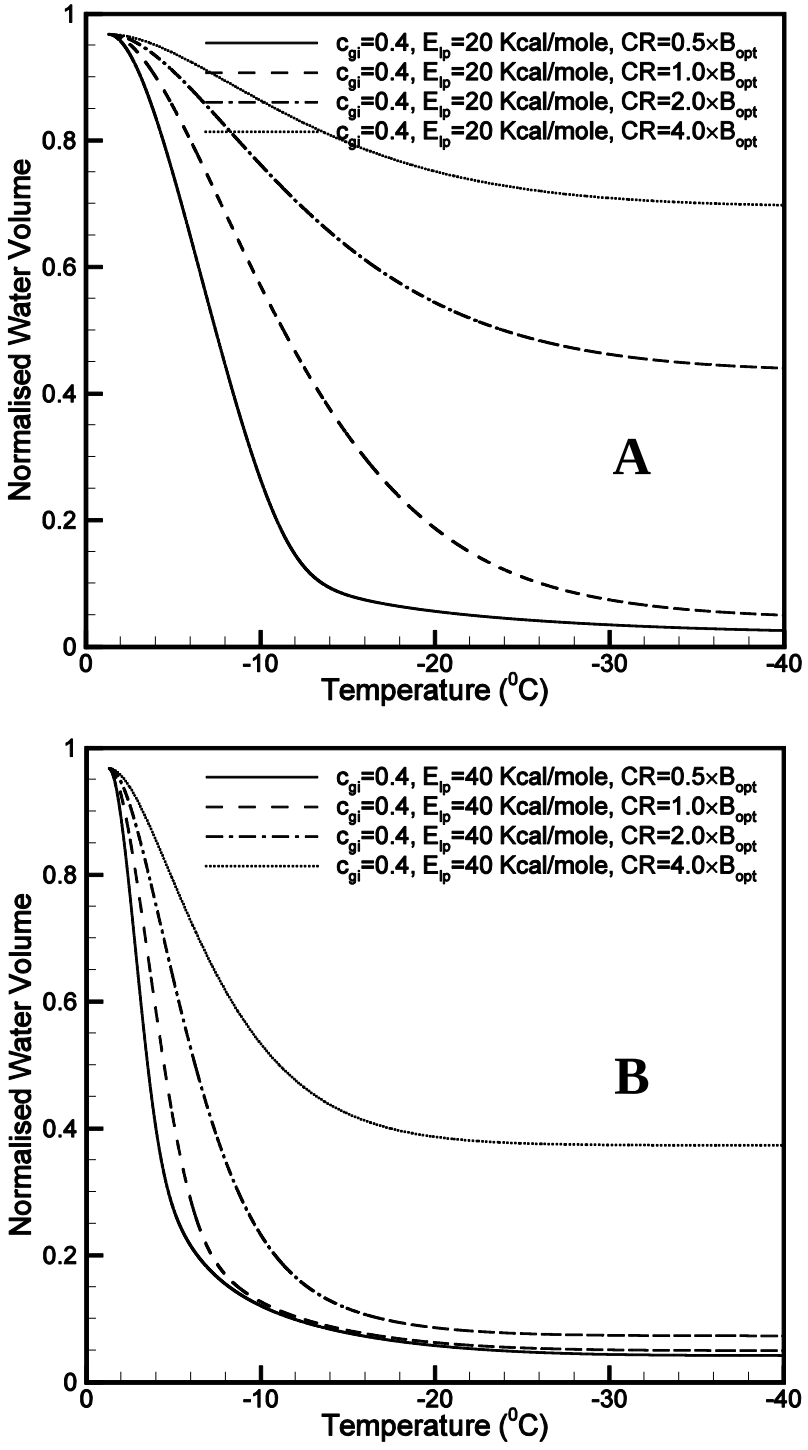

Figure 3.12: Variation of normalised water volume with temperature at $c_{gi} = 0.4M$, E_{Lp}= 20 Kcal/mole (A) and E_{Lp}= 40 Kcal/mole (B)

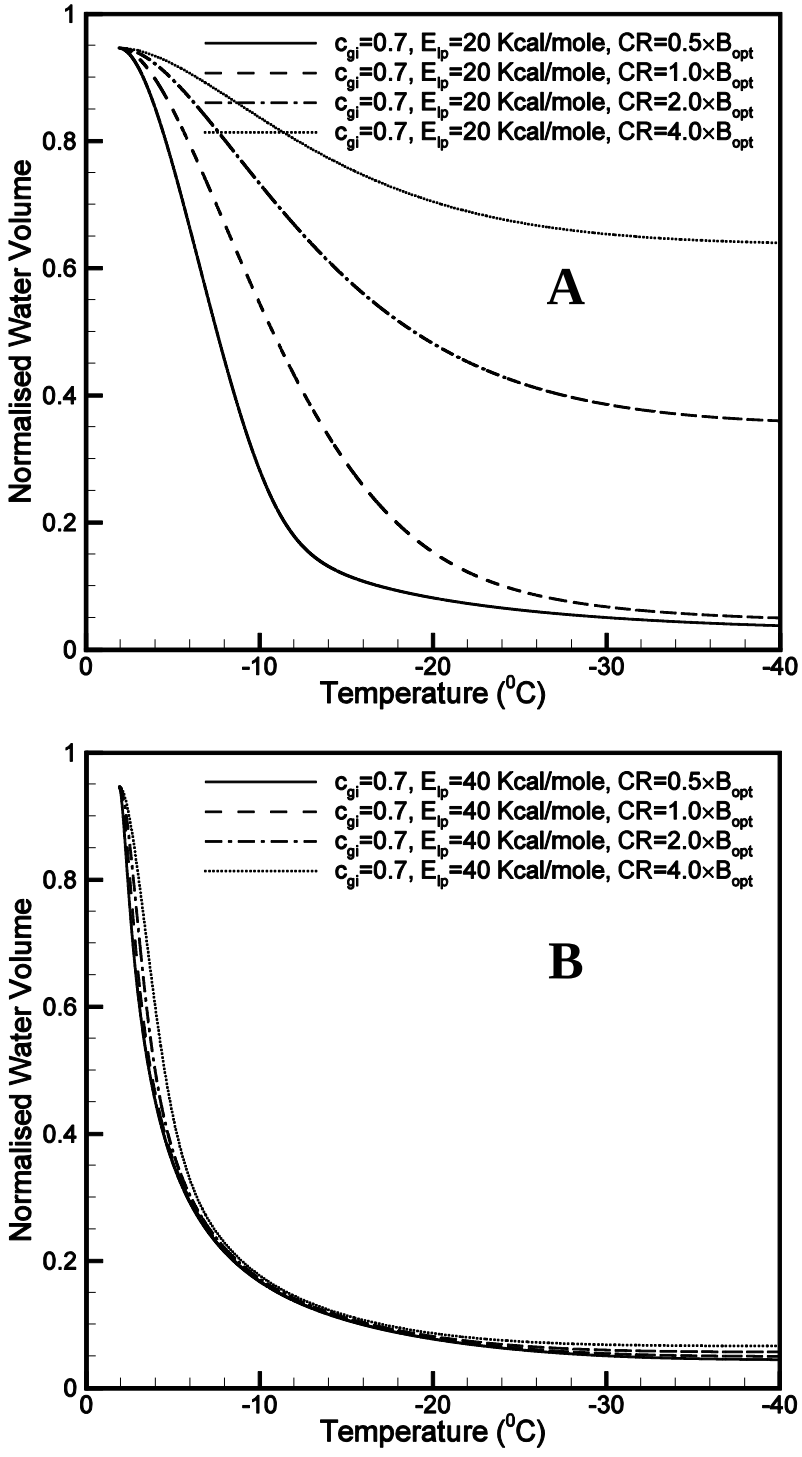

Figure 3.13: Variation of normalised water volume with temperature at $c_{gi} = 0.7M$, E_{Lp}= 20 Kcal/mole (A) and E_{Lp}= 40 Kcal/mole (B)

Figure 3.14 shows the variation of normalised water volume with temperature for cell activation energies 20 Kcal/mole and 40 Kcal/mole and cooling rates of 0.5× B_{opt}, 1.0× B_{opt}, 2.0× B_{opt}, and 4.0× B_{opt}. The freezing point gets further depressed to -2.5^{0}C because of the increase in the initial concentration of DMSO to 1.0M. For this case, all the curves for different cooling rates are collapsed into a single one, corresponding to the optimal cooling rate, for cells with high activation energy (figure 3.14 B) suggesting that the range of cooling rate for which maximum survivability can be achieved increases further as compared to the previous case. Also, for cells with low activation energy (figure 3.14 A), the trapped water volume at the end of the preservation process is almost ~5% of the initial intracellular water content for the cells cooled between 0.5× B_{opt} and 2.0× B_{opt}. This indicates that with increase in the initial DMSO concentration to 1.0M, even for the cells with low activation energy, the chances for getting higher survivability has been increased. Although, the end normalised water volume is almost same but the variation is different in the beginning of the process. For c_{gi}= 1.3M (figure 3.15) there is no difference between the two plots although the parameters for both A and B are different. And the similar trend was observed in figure 3.5 (for DMSO) and figure 3.10 (for salt). For this case also there is no influence of cooling rate and activation energy on the water transportation across the cell membrane. Hence it can be concluded that after a certain extent the cell response is not affected by the cooling rate, concentration of CPA, and cell activation energy. The numerically predicted optimal cooling rate for the studied cases is listed in Table 2. It should be noted that the simulation has been performed till the cooling rate falls below 0.001 ^{0}C/min. As mentioned earlier, it can be noticed that the optimal cooling rate decreases with the increase in cell activation energy as well as with the increase in initial DMSO concentration. Also, the variation is not linear.

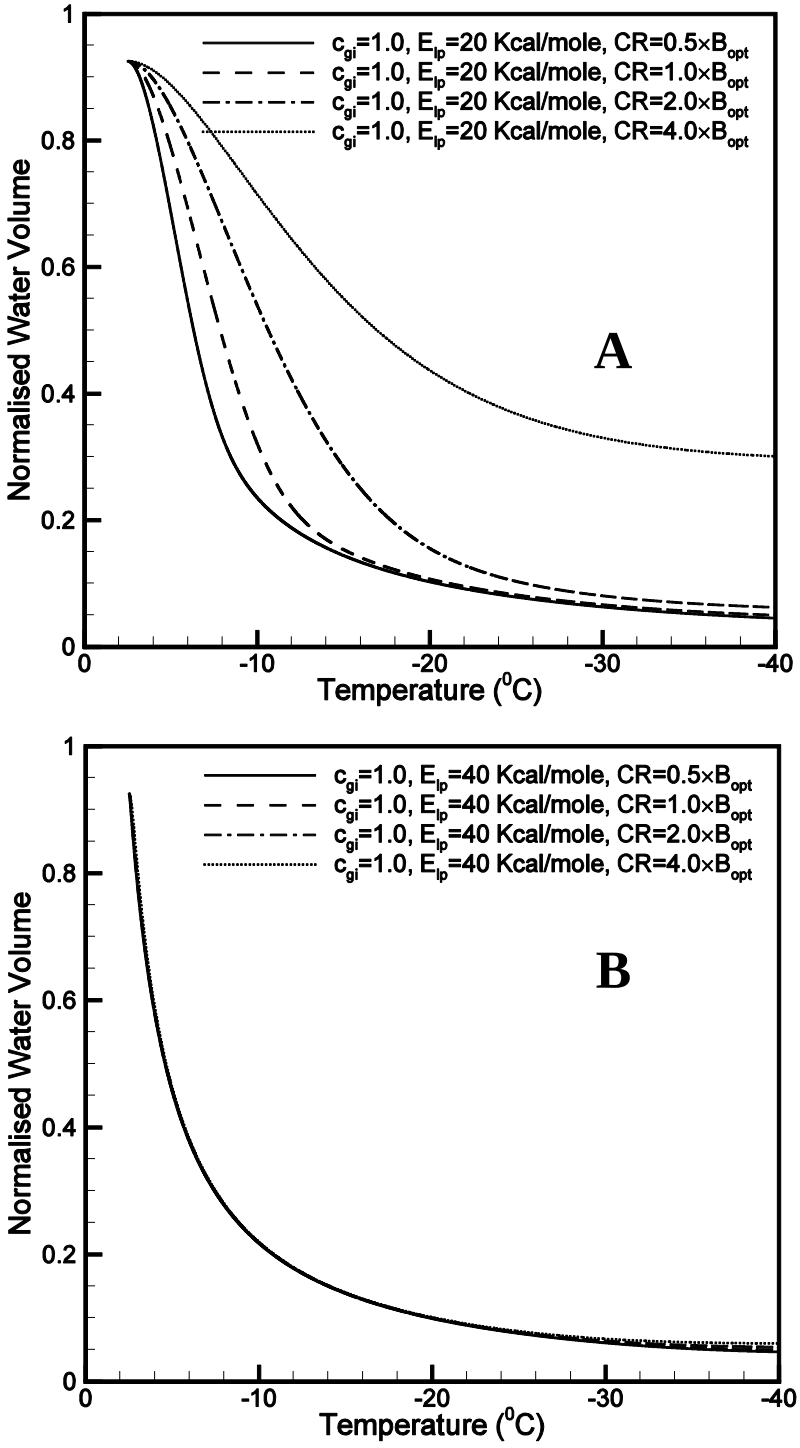

Figure 3.14: Variation of normalised water volume with temperature at $c_{gi} = 1M$, E_{Lp}= 20 Kcal/mole (A) and E_{Lp}= 40 Kcal/mole (B)

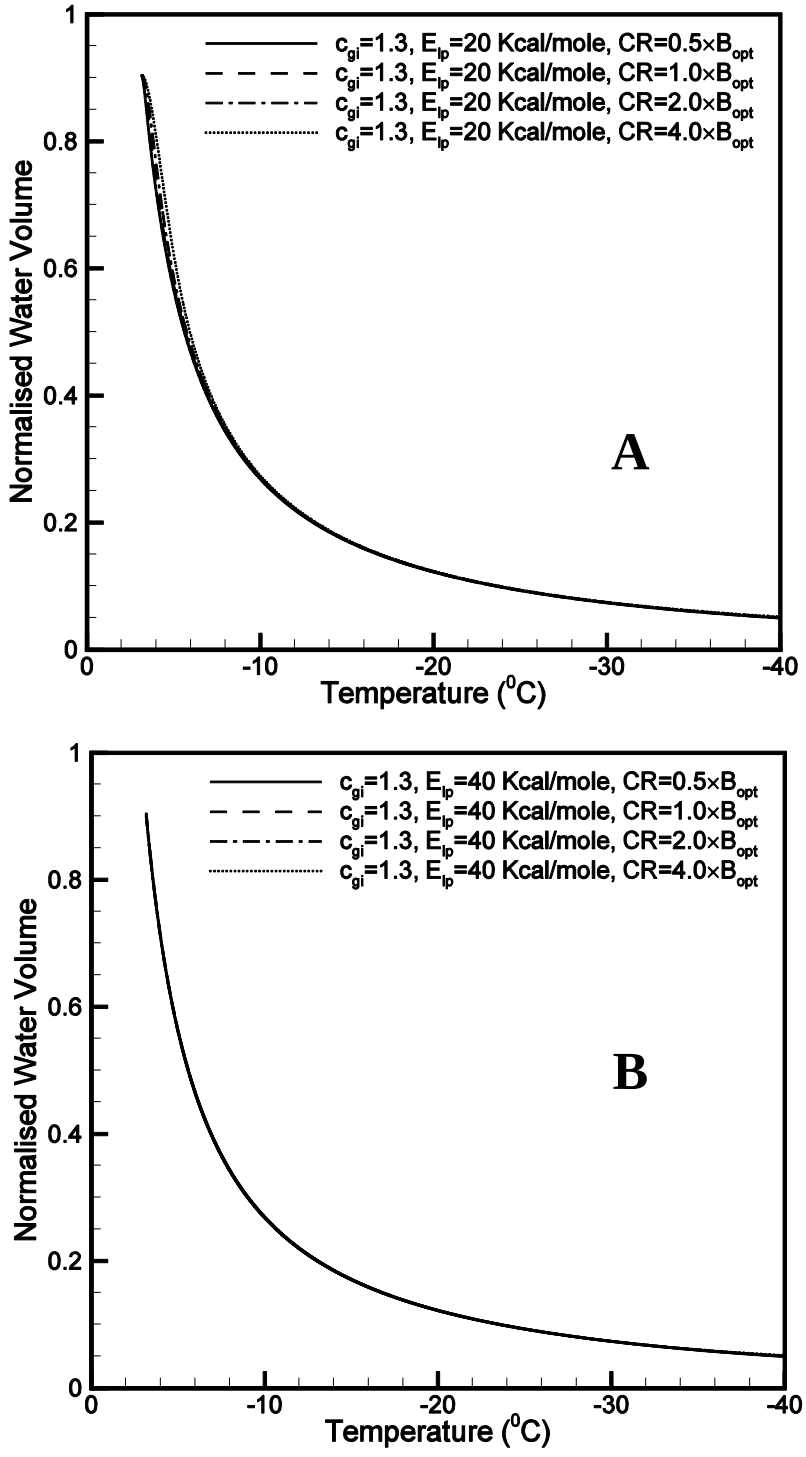

Figure 3.15: Variation of normalised water volume with temperature at $c_{gi} = 1.3M$, E_{Lp}= 20 Kcal/mole (A) and E_{Lp}= 40 Kcal/mole (B)

Table 2: Predicted optimal cooling rate at L_{pg} = 1 μm/min-atm, SA/WV=10 μm^{-1}

E_{LP} (Kcal/mole) \ c_{gi} (M)	0.1	0.2	0.3	0.4	0.5	0.6	0.7	0.8	0.9	1.0	1.1	1.2	1.3
20	4967.7	4734.8	4496.9	4251.2	3992.7	3711.2	3383.9	2938.0	2183.0	1388.1	789.0	353.0	45.85
25	3147.6	2954.8	2755.8	2544.8	2308.7	2008.1	1522.3	989.6	612.7	358.0	188.8	78.8	9.53
30	2125.8	1958.8	1780.9	1575.7	1279.9	832.3	501.8	295.3	168.5	91.4	44.9	17.5	1.98
35	1503.6	1352.6	1178.0	908.0	530.7	295.0	161.7	87.4	46.1	23.2	10.65	3.88	0.41
40	1099.3	955.2	743.1	407.0	206.6	103.9	51.95	25.76	12.5	5.87	2.52	0.863	0.0851
45	822.3	670.7	380.0	175.9	80.34	36.63	16.7	7.59	3.41	1.485	0.594	0.193	0.0175
50	622.9	426.7	183.5	76.0	31.3	12.94	5.38	2.24	0.92	0.374	0.14	0.0421	0.00367
55	471.0	234.5	88.5	32.9	12.24	4.59	1.73	0.663	0.253	0.094	0.033	0.0093	
60	341.9	127.0	42.8	14.3	4.8	1.63	0.563	0.1967	0.069	0.0238	0.0077	0.00206	
65	220.3	68.7	20.72	6.23	1.89	0.584	0.183	0.0585	0.0188	0.006	0.0018		
70	134.7	37.25	10.07	2.71	0.748	0.209	0.0598	0.0175	0.0052	0.00152			
80	50.0	11.0	2.39	0.526	0.118	0.0272	0.0064	0.0016					

Correlation for Optimal Cooling Rate

Table 2 lists the predicted optimal cooling rate for the studied parameters. Based on the prediction of optimal cooling rate, B_{opt}, for initial DMSO concentration varying between 0.1M and 1.3M, a correlation has been established which relates the optimal cooling rate with initial concentration of DMSO and the cell activation energy. It should be noted here that the optimal cooling rate is linearly dependent on reference membrane permeability L_{pg} and available surface area to water volume ratio SA/WV (results not shown) as observed in chapter 2 when DMSO was not present inside the cell. Also, the optimal cooling rate, B_{opt}, is obtained with keeping L_{pg}=1μm/min-atm and SA/WV=10 μm^{-1}. Hence, the actual optimal cooling rate, B_{opt}^{a}, for a cell line is obtained by multiplying the optimal cooling rate with the reference membrane permeability, L_{pg}, and the one-tenth times the available surface area to water volume ratio of that cell. It has been observed that the variation of optimal cooling rate does not follow a single trend with the increase in initial concentration of DMSO. So, three different regimes have been identified where the variation is similar. The three different regimes are: 0.1M ≤ c_{gi} ≤ 0.7M, 0.7M ≤ c_{gi} ≤ 0.9M, and 0.9M ≤ c_{gi} ≤ 1.3M. The developed correlations are given below,

a) **For 0.1M ≤ c_{gi} ≤ 0.7M**

$$B_{opt} = \frac{a}{10^{b}} \qquad (12)$$

$$a = A + B\times c_{gi} + C\times c_{gi}^{2} + D\times c_{gi}^{3} + E\times c_{gi}^{4}$$

$$b = Term^{1}\times (E_{Lp} - 20)^{Term^{2}}$$

$$Term^{1} = A_1 + B_1\times c_{gi} + C_1\times c_{gi}^{2} + D_1\times c_{gi}^{3} + E_1\times c_{gi}^{4} + F_1\times c_{gi}^{5}$$

$$Term^{2} = A_2 + B_2\times c_{gi} + C_2\times c_{gi}^{2} + D_2\times c_{gi}^{3} + E_2\times c_{gi}^{4} + F_2\times c_{gi}^{5}$$

A = 5186.628	A_1 = 0.034	A_2 = 0.631
B = -2085.920	B_1 = 0.019	B_2 = 5.684
C = -1290.005	C_1 = -1.726	C_2 = -15.039
D = 2711.121	D_1 = 8.767	D_2 = 2.659
E = -2666.672	E_1 = -15.118	E_2 = 31.497
	F_1 = 8.926	F_2 = -27.769

b) **For 0.7M ≤ c_{gi} ≤ 0.9M**

$$B_{opt} = \frac{a}{10^b} \qquad (13)$$

$$a = A \times e^{(B \times c_{gi} + C \times c_{gi}^2 + D \times c_{gi}^3)}$$

$$b = A_s \times X \times c_{gi}^{D_s} + B_s \times X^2 \times c_{gi}^{E_s} + C_s \times X^3 \times c_{gi}^{F_s}$$

Where $X = E_{Lp} - 20$

A = 2.44447×10^7	$A_s = 1.16757 \times 10^{-1}$
B = -3.6168×10^1	$B_s = 4.19681 \times 10^{-4}$
C = 5.05437×10^1	$C_s = -7.64367 \times 10^{-6}$
D = -2.42973×10^1	$D_s = 8.92043 \times 10^{-1}$
	$E_s = 5.34628 \times 10^{-1}$
	$F_s = 2.89983$

c) **For 0.9M ≤ c_{gi} ≤ 1.3M**

$$B_{opt} = [-4.31 \times 10^5 + 1.8467 \times 10^6 \times c_{gi} - 1.163 \times 10^6 \times c_{gi}^2] \times e^{\{c_{gi}^{0.6088} \{-0.2578 \times E_{Lp} - 0.000291 \times E_{Lp}^2\}\}} \qquad (14)$$

The actual optimal cooling rate is given as,

$$B_{opt}^a = B_{opt} \times \left\{ \left[\frac{(SA/WV)}{10} \right] \times [L_{pg}] \right\} \qquad (15)$$

The decay of optimal cooling rate is logarithmic with increase in the activation energy. This may be attributed to the fact that with increase in the activation energy, the tendency of water molecules to come out of the cell increases rapidly. The above correlation is presented in figure 3.16, 3.17 and 3.18 for $0.1M \leq c_{gi} \leq 0.7M$, $0.7M \leq c_{gi} \leq 0.9M$, and $0.9M \leq c_{gi} \leq 1.3M$ respectively at a reference membrane permeability of L_{pg}= 1μm/min-atm and the ratio of the available surface area for water transport to the initial volume of intracellular water SA/WV=10μm^{-1}. It can be noted that the optimal cooling rates computed numerically and the optimal cooling rates predicted using the established correlation, in the presence of DMSO, are matching quite well.

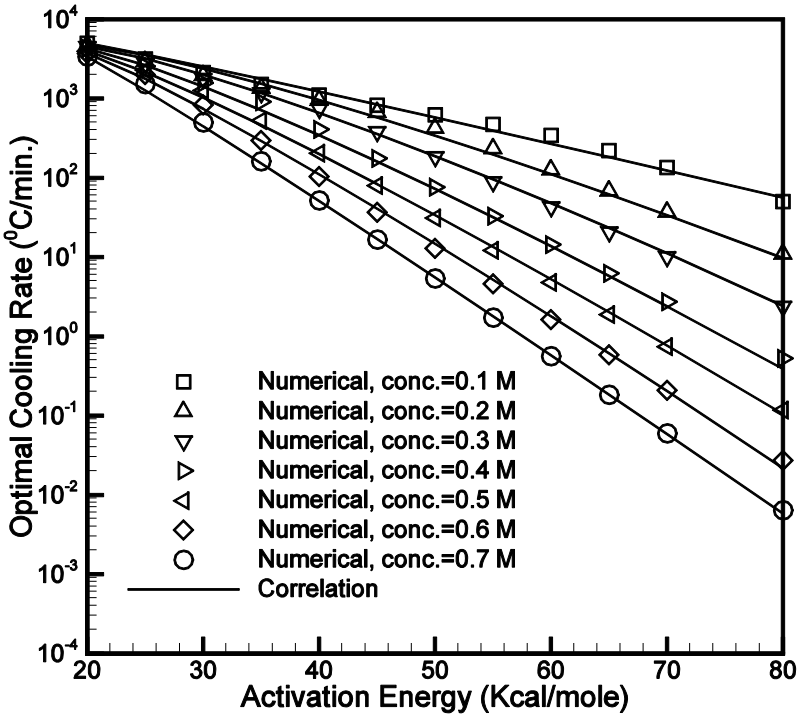

Figure 3.16: Correlation between the activation energy and optimal cooling rate for $0.1M \leq c_{gi} \leq 0.7M$, L_{pg} =1μm/min-atm and SA/WV=10 μm^{-1}

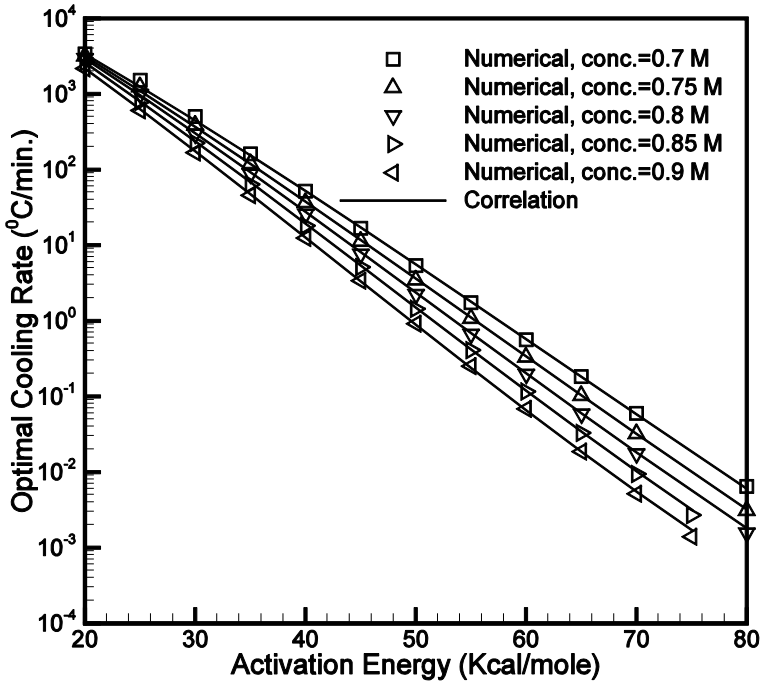

Figure 3.17: Correlation between the activation energy and optimal cooling rate for $0.7M \leq c_{gi} \leq 0.9M$, L_{pg} =1µm/min-atm and SA/WV=10 μm^{-1}

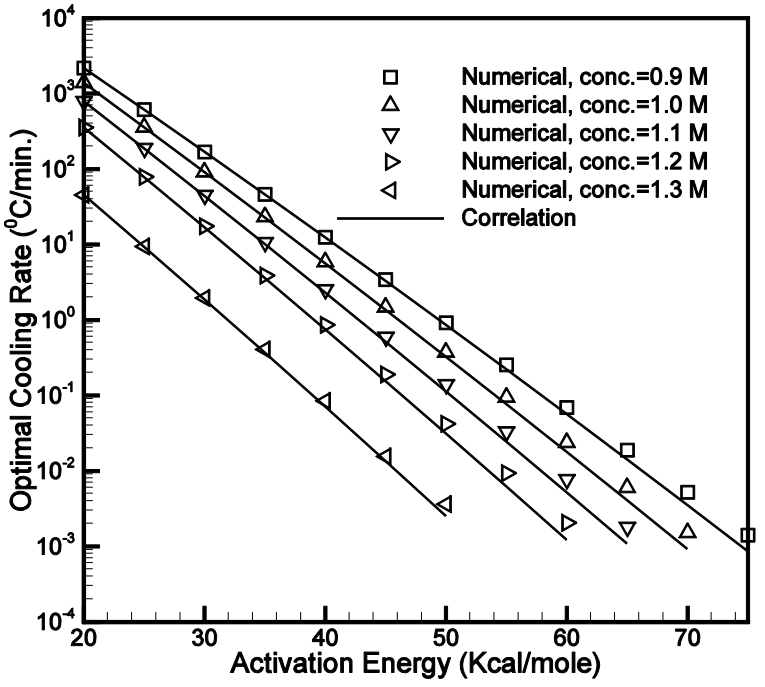

Figure 3.18: Correlation between the activation energy and optimal cooling rate for $0.9M \leq c_{gi} \leq 1.3M$, L_{pg} =1µm/min-atm and SA/WV=10 μm^{-1}

The predicted optimal cooling rate by the correlation is compared with the published experimental results. The comparison is provided in Table 3. For example, the optimal cooling rate for human lymphocyte is calculated as follows:

The input parameters are,

$L_{pg} = 0.1\mu m/(min - atm)$, $E_{lp} = 15.5\ Kcal/mole$, ${}^{SA}/_{WV} = 0.735\mu m^{-1}$, $c_{gi} = 1.0M$.

Since the initial concentration of DMSO is equal to 1.0 hence the correlation for 0.9M≤ c_{gi}≤1.3M (Equation 14) should be used.

With the given input parameters of human lymphocyte, equation (14) gives the $B_{opt} = 4333.56^0 C/min$. After putting this value in equation (15) along with the actual values of L_{pg} and ${}^{SA}/_{WV}$, $B^a_{opt} = 31.85^0 C/min$.

It should be stressed here that, although, the correlation is given for E_{Lp} values varying between 20 Kcal/mole and 80 Kcal/mole, the correlation predicts the optimal cooling rate reasonably well even for the cell activation energy below 20 Kcal/mole (as noted in the first four rows of the table). The maximum percentage error is 14% when the cell activation energy is 9.0 Kcal/mole; this error reduces to 7% when the cell activation energy is changed to 29.2 Kcal/mole.

Table 3: Comparison between the optimal cooling rates obtained experimentally and using the present correlation in the presence of CPA

Cell Type	L_{pg} μm/min -atm	E_{Lp} Kcal/mole	SA/WV	c_{gi} M	B_{opt} ^{0}C/min Reported	B_{opt}^a ^{0}C/min	%Error with B_{opt}^a	Ref.
Mouse Ova	0.044	13.3	0.096	1.0	4	3.52	12	[2], [46]
Haploid Oyster sperm	0.0015	9.1	22.02	1.02	44	49.35	-12.15	[51]
Diploid Oyster sperm	0.0019	9.0	16.86	1.02	43	49.25	-14.53	[51]
Human Lymphocyte	0.1	15.5	0.735	1.0	30	31.85	-6.16	[2], [46]
Mouse sperm	0.01	29.2	11.1	0.1	32	29.62	7.43	[58], [59]

3.5 CONCLUSION

The effect of DMSO concentration on the optimal cooling rate is studied for different values of cell activation energies. It was found that there is a decrease in the optimal cooling rate with the increase in the value of cell activation energy and also with the increase in the initial concentration of DMSO inside the cell. The study is carried out at different initial DMSO concentration (c_{gi}) values ranging from 0.1M to 1.3M and it is observed that the chances of having maximum survivability increase with the increase in DMSO concentration; because, the range of favourable cooling rate increases with the increase in DMSO concentration. This characteristic is more pronounced with the cells having higher activation energy. Also, a correlation formula is established for predicting the optimal cooling rate of a biological cell in the presence of DMSO with a goodness of fit 99.8%.

REFERENCES

[1] Mazur, P., Cryobiology: The freezing of biological systems, Science, Vol. 168, pp. 939-949, 1970.

[2] Mazur, P., Freezing of Living Cells: Mechanisms and Implications, American Journal of Physiology, 247, pp. C125–C142, 1984.

[3] Farrant, J., General observations on cell preservation. In: M.J. Ashwood-Smith and J. Farrant, Eds. Low Temperature Preservation in Medicine and Biology, Pitman Medical Limited, Kent, England, pp. 1-18, 1980.

[4] Spallanzani, L., Osservation e spezieninternoai vermicelli spermatici dell' uomo e deglianimali, Inopusculi di fisicaAnimale e Vegatabile, Opuculo II. Modeena, Italy (cited in Brotherton, 1990), 1776.

[5] Polge, C., Smith, A.U. and Parkes, A.S., Revival of spermatozoa after vitrification and dehydration at low temperatures. Nature, pp.164:666, 1949.

[6] Mazur, P., Seki, S., Pinn, I.L., Kleinhans, F.W. and Edashige, K. Extra and intracellular ice formation in mouse oocytes, Cryobiology, vol. 51, pp. 29-53, 2005.

[7] Bernard, A. and Fuller, B.J., Cryopreservation of human oocytes: a review of current problem and perspectives. Human Reproduction Update 2, pp. 193–207, 1996.

[8] Hubel, A., Parameters of cell freezing: implications for the cryopreservation of stem cells, Transfusion Medicine Reviews, vol. 11, pp. 224-233, 1997.

[9] Day, S. H., Nicoll-Griffith, D. A. and Silva, J. M., Cryopreservation of rat and human liver slices by rapid freezing, Cryobiology, Vol. 38, pp. 154-159, 1999.

[10] Oegema, T. R., Deloria, L. B., Fedewa, M., Bischof, J. C. and Lewis, J. L., A simple cryopreservation method for the maintenance of cell viability and mechanical integrity of cultured cartilage analogy, Cryobiology, Vol. 40, pp. 370-375, 1999.

[11] Lovelock, J.E., Biophysical aspects of the freezing and thawing of cells, The journal of the Royal Society of Medicine, vol. 47, pp. 60-62, 1954.

[12] Mazur, P., Kinetics of Water Loss from Cells at Subzero Temperatures and the Likelihood of Intracellular Freezing, Journal of General Physiology, vol. 47, pp. 347– 369, 1963.

[13] Mazur, P., Studies on rapidly frozen suspensions of yeast cells by differential thermal analysis and conductometry, Biophysical journal, vol. 3, pp. 323-353, 1963.

[14] Bank, H. and Mazur, P., Visualization of freezing damage, The Journal of Cell Biology, Vol. 57, pp. 729 -742, 1973.

[15] Mazur, P., Leibo, S. P., and Chu, E. H. Y., A Two Factor Hypothesis of Freezing Injury, Exp. Cell Res., vol. 71, pp. 345–355, 1972.

[16] Muldrew, K. and McGann, L.E., The Osmotic rupture hypothesis of Intracellular Freezing Injury, Biophysical journal, Biophysical society, vol. 66, pp. 532-541, February 1994.

[17] Muldrew, K. and McGann, L.E. Mechanism of intracellular ice formation, Biophysical journal, Biophysical society, vol. 57, pp. 525-532, March 1990.

[18] Karlsson, J.O.M., Cravalho, E.G., and Toner, M., A model of diffusion-limited ice growth inside biological cells during freezing, Journal of Applied Physiology; vol. 75, pp. 4442–4455, 1994.

[19] Devireddy, R. V., Raha, D. and Bischof, J. C., Measurement of water transport during freezing in cell suspensions using a differential scanning calorimeter, Cryobiology, Vol. 36, pp. 124-155, 1998.

[20] Devireddy, R. V. and Bischof, J. C., Measurement of water transport during freezing in mammalian liver tissue - Part II: The use of differential scanning calorimetry, ASME Journal of Biomechanical Engineering, Vol. 120, pp. 559-569, 1998.

[21] Devireddy, R. V., Coad, J. E. and Bischof, J. C., Microscopic and calorimetric assessment of freezing processes in uterine fibroid tissue, Cryobiology, Vol. 42, pp. 225-243, 2001.

[22] Devireddy, R. V. and Bischof, J. C., Recent Advances in Cryobiology Using Calorimetry, In: S. Kakac, H. Smirnov and M.R. Mila (eds.), Low Temperature and Cryogenic Refrigeration, Kluwer Academic Publishers, Dordrecht, The Netherlands, pp. 265-294, 2003.

[23] Diller, K. R., and Cravalho, E. G., A Cryomicroscope for the Study of Freezing and Thawing Process in Biological Systems, Cryobiology, vol. 7, pp. 191–199, 1970.

[24] Devireddy, R. V., Swanlund, D. J., Roberts, K. P., Pryor, J. L. and Bischof, J. C., The effect of extracellular ice and cryoprotective agents on the water permeability parameters of human sperm plasma membrane during freezing, Human Reproduction, Vol. 15, pp. 1125-1135, 2000.

[25] Devireddy, R. V., Olin, T., Vincente, W., Troedsson, M. H. T., Bischof, J. C. and Roberts, K. P., Cryopreservation of equine spermatozoa: Optimal cooling rates in the presence and absence of cryoprotective agents, Biology of Reproduction, Vol. 66, pp. 222-231, 2002 (a).

[26] Devireddy, R. V., Brooke, F., Godke, R. A. and Leibo, S. P., Subzero water transport characteristics of boar spermatozoa confirm observed optimal cooling rates, Molecular Reproduction and Development, Vol. 67, pp. 446-457, 2004.

[27] Diller, K. R., Quantitative Low Temperature Optical Microscopy of Biological Systems, Journal of Microscopy, vol. 126, pp. 9–28, 1982.

[28] Du, J., Tao, J., Kleinhans, F. W., Mazur, P. and Critser, J. K., Water volume and osmotic behavior of mouse spermatozoa determined by electron paramagnetic resonance, Journal of Reproduction & Fertility, Vol. 101, pp. 37-42, 1994.

[29] Jacobs, M.H., The simultaneous measurement of cell permeability to water and to dissolved substances. Journal of Cellular and Comparative Physiology, vol. 2, pp. 427-444 (1932-1933).

[30] Kedem, O., and Katchalsky, A., Thermodynamic analysis of the permeability of biological membranes to non-electrolytes. Biochimicaet BiophysicaActa., vol. 27, pp. 229-246, 1958.

[31] Levin, R. L., Cravalho, E. G., and Huggins, C. G., A Membrane Model Describing the Effect of Temperature on Water Conductivity of Erythrocyte Membranes at Subzero Temperatures, Cryobiology, vol. 13, pp. 415–429, 1976.

[32] Kasharin, A.V., and Karlsson, J.K., Analysis of mass transport during warming of cryopreserved cells. Annals of the New York Academy of Sciences, vol. 858, pp. 163-174, 1998.

[33] Mazur, P., Causes of injury in frozen and thawed cells, Fed. Proc. 24, Suppl. 15, pp. S-175- 182, 1965.

[34] Mazur, P., in Cryobiology, H. T. Meryman, Ed. (Academic Press, New York, 1966), pp. 213-315.

[35] Van den Berg, L., Arch. Biochem. Biophys.84, 305 (1959), Cryobiology, vol. 3, 236 (1966); and F. S. Soliman, ibid. 6, 10 (1969).

[36] Mazur, P. and Schmidt, J.J., Interactions of cooling velocity, temperature and warming velocity on the survival of frozen and thawed yeast, Cryobiology, vol. 5, pp. 1-17, 1968.

[37] Leibo, S. P., Farrant, J., Mazur, P., Hanna, M., G., and Smith, L. H., Effect of freezing on marrow stem cell suspensions: interactions of cooling and warming rates in the presence of PVP, sucrose or glucose, Cryobiology, vol. 6, pp. 315 – 332, 1970.

[38] Mazur, P., Rhian, M.A., Mahlandt, B. G., Arch. Biochem. Biophys. 71, 31 (1957); R.D. Goos, E. E. Davis, W. Butterfield, Mycologia 59, 58 (1967); J. K. Koehler, Cryobiology, vol. 3, pp. 392, 1967.

[39] Karlsson, J.O.M. and Toner, M., Long term storage of tissues by cryopreservation: Critical issues, Biomaterials, vol. 17, pp. 243–256, 1996.

[40] Arakawa, T., Carpenter, J. F., and Crowe, J. H., Basis for toxicity of certain cryoprotectants: a hypothesis. Cryobiology, vol. 27, pp. 401-415, 1990.

[41] Karlsson, J. O. M., Cravalho, E. G., Borel, R. I., Tompkins, R. G., Yarmush, M. L., and Toner, M., Nucleation and growth of ice crystals inside cultured hepatocytes during freezing in the presence of dimethylsulfoxide, Biophysics Journal, Vol. 65, pp. 2524-2536, 1993.

[42] McGee, H. A. Jr., and Martin, W., J., Cryochemistry, Cryogenics, vol. 2, pp.1-11, 1962.

[43] Rice, F. O., History of radical trapping, Information and trapping of free radicals, edited by A., M., Bass, and H., P., Broida, New York, Academic, p7, 1970.

[44] Liniger, W., Zur Stabilitat der numerischen Integrations-methoden fur Differential gleichungen. Doctoral thesis, University of Lausanne, Zurich, 1957.

[45] Karim, A. I. A., The Stability of Fourth Order Runge-Kutta Method for the Solutions of Systems of Differential Equations, Communications of the ACM, vol. 9, No. 2, pp. 113-116, 966

[46] Thirumala, S. and Devireddy, R. V., A simplified procedure to determine the optimal cooling rate of freezing biological systems, Journal of Biomechanical Engineering, Vol. 127, pp. 295-300, 2005.

[47] Rasmussen, D.H., Macaulay, M.N. and Mackenzie, A.P., Supercooling and nucleation of ice in single cells, Cryobiology, Vol. 12, pp. 328-339, 1975.

[48] Franks, F., Mathias, S.F., Galfre, P., Webster, S.D. and D.Brown, Ice nucleation and freezing in undercooled cells, Cryobiology, Vol. 20, pp. 298-309, 1983.

[49] George, M. F., Becwar, M. R. and Burke, M. J., Freezing avoidance by deep undercooling of tissue water in winter-hardy plants, Cryobiology, Vol. 19, pp. 628-639, 1982.

[50] Pinisetty, D., Huang, C., Dong, Q., Tiersch, T., R., Devireddy, R. V., Subzero water permeability parameters and optimal freezing rates for sperm cells of the southern platyfish Xiphophorus maculatus, Cryobiology, Vol. 50, pp. 250-263, 2005.

[51] He, Y., Dong, Q., Tiersch, T., R., Devireddy, R. V., Variation in the membrane transport properties and predicted optimal rates of freezing for spermatozoa of diploid and tetraploid pacific oyster, Crassostrea gigas, biology of reproduction, vol. 70, pp.1428-1437,2004.

[52] Thirumala, S., Huang, C., Dong, Q., Terrence, R., T., Devireddy, R., V., A theoretically estimated optimal cooling rate for the cryopreservation of sperm cell from a live bearing fish, the green swordtail, Xiphophorus helleri, Theriogenology, vol. 63, 2005, pp.2395-2415

[53] G. Li, J. Saenz, R. A. Godke, R. V. Devireddy, Effect of glycerol and cholesterol loaded cyclodextrain on freezing induced water loss in Bovine spermatozoa, Reproduction, DOI: 10.1530/rep.1.00995, pp. 875-886, 2006.

[54] Thirumala, S., Ferrer, M.S., Al-Jarrah, A., Eilts, B.E., Paccamonti, D.L. and Devireddy, R., V., Cryopreservation of canine spermatozoa: theoretical prediction of optimal cooling rates in the presence and absence of cryoprotective agents, Cryobiology, vol. 47, pp. 109 – 124, 2003.

[55] Fujikawa, S., The effect of various cooling rates on the membrane ultrastructure of frozen human erythrocytes and its relation to the extent of haemolysis after thawing, journal of Cell Science, vol. 49, pp. 369-381, 1981.

[56] Mazur, P., The role of intracellular freezing in the death of cells cooled at supraoptimal rates, Cryobiology, vol. 14, pp. 251-272, 1977.

[57] Scheiwe, M.W., Nick, H.E. and Korber, C., An experimental study on the freezing of red blood cells with and without hydroxyethyl starch, Cryobiology, vol. 19, pp. 461- 477, 1982.

[58] Devireddy, R.V., Swanlund, D.J., Roberts, K.P. and Bischof, J.C., Subzero water permeability parameters of mouse spermatozoa in the presence of extracellular ice and cryoprotective agents, Biology of Reproduction, vol. 61, pp. 764–775, 1999.

[59] Hagiwara, M., Choi, J. H., Devireddy, R.V., Roberts, K., Wolkers, W.F., Makhlouf, A. and Bischof, J.C., Cellular biophysiology during freezing of Rat & Mouse sperm predicts post that motility, Biology of Reproduction, vol. 81, pp. 700-709, 2009.

[60] Henry, M. A., Noiles, E. E., Gao, D., Mazur, P., and Critser, J. K., Cryopreservation of Human Spermatozoa. IV. The Effects of Cooling and Warming Rate on the Maintenance of Motility, Plasma Membrane Integrity and Mitochondrial Function, Fertil. Steril. Vol. 60, pp. 911–918, 1993.

[61] Toner, M. and Cravalho, E.G., Thermodynamics and kinetics of intracellular ice formation during freezing of biological cells, Journal of Applied Physiology, vol. 67 (3), pp. 1582-1593, February 1990.

[62] Toner, M., Cravalho, E.G., and Armant, D.R., Water transport and estimated transmembrane potential during freezing of mouse oocytes, Journal of membrane biology, vol. 115, pp. 261-271, 1990.

[63] Mazur, P., Equilibrium, Quasi-Equilibrium, and Non-equilibrium Freezing of Mammalian Embryos, Cell Biophysics, vol. 17, pp. 53–92, 1990

Vita

The author was born in Dhenkanal, Odisha on 31st May 1987. She got her secondary education from Brajanath Badajena High School, Dhenkanal, Odisha, India. She did her Intermediate degree from Baxi Jagabandhu Bidyadhara Junior College, Bhubaneswar, Odisha, India in 2004. She received the degree of Bachelor of Technology in Biotechnology Engineering from Gandhi Institute of Engineering and Technology, Gunupur, Odisha, India in 2009. She is a candidate for the degree of Master of Technology in Biotechnology and Medical Engineering at National Institute of Technology, Rourkela, Odisha, India. After completing her master's degree she would be pursuing her doctoral program.

Journals

D. Devismita, A. Kumar, Effect of cryoprotectant on optimal cooling rate during cryopreservation, Cryobiology (2014), http://dx.doi.org/10.1016/j.cryobiol.2014.12.002

Conferences

[1] Devismita D. and Kumar A., Effect of cryoprotectant on Optimal Cooling Rate during Cryopreservation, in Proceedings: 2nd International Conference on Biomedical Engineering and Assistive Technologies, BEATs, December, 2012, ISBN-13: 978-81-925454-1-7, pp. 166-169.

[2] Devismita D. and Kumar A., Effect of Permeability Parameters on the Optimal Cooling Rate of Biological Systems, in Proceedings: 2nd International Conference on Biomedical Engineering and Assistive Technologies, ICMSDPA, October, 2012.

[3] Devismita D., Kumar A. and Ramajayam K.K., Cryopreservation of Human Sperm: Effect of Cooling Rate on Intracellular Ice Formation, in Proceedings: International Conference on Emerging Trends, ICET, March, 2012.

[4] Devismita D. and Kumar A., Cryopreservation of Equine Sperm: Effect of Cooling Rate on Intracellular Ice Formation, in Proceedings: International Conference on Mathematical Modelling and Application to Industrial Problems, MMIP, March, 2011.